Emergent Properties of Spike-Frequency Adaptation in Neuronal Systems: Non-renewal statistics, Variability Reduction and Sparsening

Inaugural-Dissertation
to obtain the academic degree
Doctor rerum naturalium (Dr. rer. nat.)

submitted to the Department of Biology, Chemistry and Pharmacy
of Freie Universität Berlin

by

Farzad Farkhooi
from Shiraz

2011

The research presented in this dissertation was carried out from January 2007 until March 2011 at Theoretical Neuroscience & Neuroinformatics group, Freie Universität Berlin, under the supervision of Prof. Dr. Martin P. Nawrot.

1^{st} *Reviewer :*	Martin P. NAWROT	-	Freie Universität Berlin & BCCN, Berlin
2^{nd} *Reviewer :*	Carl VAN VREESWIJK	-	René Descartes University & CNRS, Paris

Date of defense: September 16, 2011

Acknowledgments

I express my deep gratitude to my Ph.D adviser, Martin P. Nawrot. He is certainly the one that let me to experience and learn by his open manner and his creative philosophy. He supervises my work in an outstanding way and generously supported me, both morally and otherwise, in his original respectful and friendly way. He taught me how to explore hidden corners of problems, thanks so much Martin.

Carl van Vreeswijk coached my staying at his lab in a rainy spring 2009, since I have knocked on his door just ask for some help and a refuge. His way of thinking influences whole a lot my work and life. I owe him gazillions of acknowledgments for his mentoring, although short, they were very intense and franc; I am hoping and counting down to work with him a bit more.

I thank Prof. Dr. Randolf Menzel for letting me to be in his group to learn biology and the great fascination of honeybee brain; I acknowledge him for many insightful and careful feedbacks. Eilif Muller has considerably contributed to the fundamentals of my thesis by his extremely interesting and cool paper. I thank him very much, hoping to continue this elegant collaboration. I thank Anja Froese; she contributed a lot by her excellent experiment. I thank Martin Stube-Bloss for our discussions and his high quality data. Thanks to all my colleagues and friends with whom I worked, Micheal Schmuker, Evern Pamir, Jan Soelter, Gundula Meckenhäuser, Chris Hausler, Thomas Rost, Joachim Haenicke and Michael Pereira. Thank you so much all for reading and correcting my ideas and writings. I also thank Aster for her best coffee, music and for being the source of hope in the middle of no-hope intervals.

I am very thankful to all of my friends, whom supported me with their love. I would like to specially thank: Wiebke Hensle for clam and active energy, Diego Maronese for ideas with structures and beyond, Vered Nethe for caring and hearing, Neloy Kumar Chakraborty for big and open heart, Melanie Sehgal for understanding and kindness, Alicia Frankovich for good words and giving energy, Alex Martinis Roe for diligence and intelligence, Leo Bazzo for being positive and everywhere, Sebastian Horndasch for sharing and compassion, Edyta Kutnik for trying and opening, Florian Hottarek for warmth and cheerfulness, Diego Chamy for joyous and thoughts, Azubuike Erinugha for wisdom and madness.

A gazillions of thanks to Jörg Heuer for his unbroken support and encouragement. I am grateful for his ideas and considerations and our wonderful late night chats.

Katharina Iva Nagel, I am very thankful for your words, supports, compassion, smiles and love. I indebted with your patience, your cheerful vivid way, your peace and your energy. My deepest gratitude to Kat for your thoughtful manner and the tasteful mango jam while having two thoughts!

Without support of my mother and father, Zhaleh and Iraj, my brother Roozbeh, and Sharyar and Leilia, it wouldn't have been possible to do this work.

While writing this dissertation many friends in Iran are suffering while fighting for their voice, our voice. My sincere gratitude goes to them and all who dream a better life.

This dissertation is based on the following manuscripts:

Serial Correlation in Neural Spike Trains: Experimental Evidence, Stochastic Modeling, and Single Neuron Variability

Authors and Contributions: Farzad Farkhooi, Martin Stube-Bloss and Martin P. Nawrot

Introduced the model and derived the equations: FF. Conceived and designed the experiment: FF, MSB and MPN. Gathered data: MSB. Analyzed the data: FF. Worte the paper: MPN and FF.

The work is peer-reviewed and published in [Farkhooi 2009b] and available at publisher website at `http://link.aps.org/doi/10.1103/PhysRevE.79.021905`.

Adaptation Reduces Variability of the Neuronal Population Code

Authors and Contributions: Farzad Farkhooi, Eilif Muller and Martin P. Nawrot

Contributed the model: EM. Derived the equations: FF. Conceived and designed the work: FF and MPN. Analyzed the data: MPN. Ran Simulations and numerical checks: FF. Wrote the paper: FF, EM and MPN.

This is a preprint of a published paper [Farkhooi 2011a] and is available at the preprint repository arXiv [Farkhooi 2011b] and accessible via `http://arxiv.org/abs/1007.3490`.

Response Adaptation Can Explain Temporally Sparse Code in the Insect Mushroom Body

Authors and Contributions: Farzad Farkhooi, Anja Froese, Eilif Muller, Randulf Menzel and Martin P. Nawrot

Introduced the model and ran the simulations : FF. Analyzed the simulated data: FF. Conceived and designed the research : FF, AF, EM, RM and MPN. Gathered data: AF. Analyzed the experimental data: MPN. Contributed the materials for simulation: EM and FF. Wrote the manuscript: FF and MPN.

The early version of this work is reviewed and published in [Farkhooi 2009a] and its supplement is available at arXiv [Farkhooi 2010]. The additional experimental material and further indepth analysis is performed in the current version and will be submitted for publication.

Zusammenfassung

Die vorliegende Arbeit trägt zum besseren Verständnis von neuronaler Spike-Frequenz Adaptation und ihrer komplexen Dynamik *in vivo* bei. Sie liefert eine detaillierte Studie über die aus der Adaptation entstehende Statistik des nicht-Erneuerungprozesses aus aufeinanderfolgenden Interspike-Intervallen. Die vorgestellten Ergebnisse zeigen, dass Spike-Frequenz Adaptation einen entscheidend positiven Effekt auf die Reduktion der Variabilität und Codierungskapazität in neuronalen Systemen hat. Darüber hinaus untersuche ich die Filterung der Adaptation in Bezug auf die Informationcodierung auf Netzwerkebene um die Emergenz einer Sparse-Code Repräsentation eines Stimulus zu beschreiben. Dieser Sparse-Code erklärt die spärliche Aktivität von intrinsischen Neuronen des Pilzkörpers der Insekten bei der Verarbeitung olfaktorischer Informationen.

Summary

This research contributes to the understanding of spike-frequency adaptation and its complex dynamics *in vivo* condition. It provides a detailed study of the non-renewal statistics emergence between subsequent inter-spike intervals due to adaptation. The results presented in this dissertation show that spike-induced adaptation has a major positive effect on the variability reduction and coding capacity in neuronal systems. Furthermore, I explore its filtering consequences on information coding at a network level to describe a mechanism for emergence of a sparse representation of the stimulus. The emerged sparse code can explain the activity of Kenyon cells in insect olfactory information processing.

Keywords: Spike-Frequency Adaptation, Point Process, Neuronal Spiking Statistics, Spiking Neuron Information Processing

Contents

Chapter 1

Introduction

Spiking neurons in the nervous system are not alike. They differ in their topological position in the network, geometrical shape and electrical properties. Despite of many differences, a fairly common feature of excitatory spiking neurons, is that cannot sustain a steady frequency of action potential production throughout a continuous steady stimulation. A common feature is that they fire rapidly at the onset of the stimulus and then slow down, even if the stimulus remains strong [Bear 2006]. This phenomenon is called spike rate or spike-frequency adaptation. Phenomenologically, spike-frequency adaptation refers to an intrinsic property of neurons that gradually decrease their activity in response to a sudden jump in their input level [Benda 2003]. It is ubiquitous in excitatory spiking neurons in many neuronal systems: it has been observed in the vast majority of excitatory neurons of diverse species alongside of the whole processing pathways of spiking neurons [Sobel 1994, Wang 1998, Sanchez-Vives 2000b, Fuhrmann 2002]. This diversity became clear by looking into the common and wide array of the biophysical mechanisms that produce spike induced adaptation. The predominant examples of those physiological mechanisms are the voltage-gated potassium currents (M-type currents) [Brown 1980] and the calcium-gated potassium channels (AHP-type currents) [Madison 1984, Schwindt 1988, Storm 1990]. Additionally, sodium-gated potassium channels [Schwindt 1989] and the slow recovery from inactivation of the fast sodium current [Fleidervish 1996] might also be responsible for spike-frequency adaptation. AHP-type currents and sodium-gated-potassium currents are mainly activated during calcium/sodium influx at each spike [Williams 1997, Bowden 2001, Yamada 2004, Goldberg 2005]. Similarly, M-type currents are mediated by high-threshold slow potassium channels, which directly rely on action potential generation mechanisms [Ermentrout 2001]. Both M-type and AHP-type currents exhibit an activation time-constant in the order of 100ms. However, the time course of adaptation caused by sodium-gated potassium time-constant is in the order of several seconds [Benda 2003].

Principally, neurons with spike-frequency adaptation operate within a highly complex network with fluctuating inputs and a large degree of heterogeneity, beyond any *in vitro* observations. Under such conditions, the long lasting effects of spike-frequency adaptation compare to a typical *in vivo* like firing statistics alter the integration dynamics of adaptive spiking cells. In this dissertation, the appearance of such complex dynamics *in vivo* neuronal activities is denoted as an *emergent property* of spike-frequency adaptation.

Emergence of Non-renewal statistics. Renewal processes such as Poisson and Gamma processes, enjoy widespread use in the literature. They have been applied to model the firing statistics of neurons receive *in vivo* like fluctuating input [Moore 1966, Perkel 1967a, Perkel 1967b, Shadlen 1998, Bastian 2001]. In the renewal theory, the firing probability is modeled as a function of the time since the last spike, or age, and successive inter-spike intervals are statistically independent [Cox 1970]. However, one significant emergent property of spiking neurons with adaptation is that they violate the fundamental assumption of inter-spike intervals independence as formulated in the canonical renewal theory. subsequent intervals of action potentials, since after each spike the underling adaptation mechanisms affect the probability of the next spike generation [Muller 2007]. Chapter 2 summarizes and collects the results on emergence of negative serial dependencies among inter-spike intervals due to spike-frequency adaptation *in vivo* conditions. Moreover, it provides an additional experimental evidence that supports the existence of negative serial interval correlations in the extrinsic neurons of Honeybee's mushroom body, so called α-lobe. The serial dependency in inter-spike intervals is quantified with the linear correlation coefficient between subsequent inter-spike intervals [Farkhooi 2009b, Benda 2010, Liu 2001, Nawrot 2008, Ávila-Åkerberg 2011]. To study serial interval correlations between adjacent inter-spike intervals and their emergent statistical property in chapter 2, a family of autoregressive point processes is introduced, where its marginal inter-spike interval distribution is described by the generalized gamma model. The generalized gamma process includes as special cases of the log-normal and gamma distributions. Those distributions have been widely used to characterize spiking neurons' statistics *in vivo*. The introduced serially correlated point process model is used to investigate that how serial interval correlations affect the distribution of the number of spikes N_T in a given time window T (so called counting process) in a numerical simulation. This distribution is of a significant importance, since it provides a description for the number of events that post-synaptic neurons receive in the time interval of T, and presumably forms the post-synaptic responses. This analysis shows that the variance of the neuronal spike counting process for the experimentally confirmed negative serial correlation is significantly reduced. Therefore, a measure of single neuron variability as quantified by the Fano factor [Fano 1947] defined as,

$$F_T = \frac{Var(N_T)}{E(N_T)} \tag{1.1}$$

is reduced by up to 50%. This result indicates that the estimation of the mean firing rate becomes more efficient and it favors the transmission of a firing rate code [Farkhooi 2009b].

Adaptation phenomenology and emergence of non-renewal statistics. The result in chapter 2 that indicates the reduction of Fano factor for a single neuron is merely due to the introduction of negative serial correlations within the series of inter-event intervals. It is shown also in [Benda 2010] almost all known phenomenological and physiological models of spike-frequency adaptation exhibit the inter-event negative serial dependencies as well. Therefore, it is of interest to study the conditions that may lead to the introduction of a non-renewal process in adaptive spiking neurons. Chapter 3 provides a set of conditions for the emergence of non-renewal statistics for neurons with spike-frequency adaptation are studied. Therein, a fairly general phenomenological model of spike-frequency adaptation in [Dayan 2001, Muller 2007] is analyzed, where adaptation self-negative feedback input x is modeled with a shot-noise dynamics

$$\dot{x} = -\tau x + q \sum \delta(t - t_k) \tag{1.2}$$

where τ is time constant of relaxation, q is the fix conductance change in the level of adaptation, δ is Dirac-delta function which has its mass at the time of t_k, where indicates the time of k^{th} spike. In a rigorously analytical treatment, it is formally shown that an adaptive process exhibits negative serial correlations if and only if (i) after an event there should be a self-inhibitory feedback, similar to Eq. (1.2), and simultaneously (ii) the probability of the occurrence of an event is increasing over time.

Adaptation at the population level. The improvement of the transmission of a rate code can be observed in many cells with spike-frequency adaptation given the emergence of negative serial correlations in their background activity. However, it is of interest to study the effect of adaptation in a population of neurons to investigate if the statistical result above (and in chapter 2) is also valid at the population level. This question is studied in chapter 3. To this end, an elegant approach introduced in [Muller 2007] for the treatment of neuronal ensembles based on a population density method is employed. The approach is based on a canonical conductance-based integrate-and-fire neuron model driven by Poisson spike trains, augmented by mechanisms for spike-frequency adaptation and a relative refractory period. In [Muller 2007], it is shown that the full five-dimensional field equation for a neuronal ensemble with the assumption of incoherent activity can be reduced to a Markov point process model by an adiabatic elimination of fast variables [Gardiner 2004]. This is a formulation that allows a development of a generalized non-renewal theory to investigate the effect of a slow adaptation variable on the expressions at the population level for (i) the count statistics and its Fano factor in an arbitrary time window, and (ii) the inter-event interval statistics, e.g. coefficient of variation C_v. Thereafter, it is proved that the system at the ensemble level also exhibits non-renewal property due to the emergence of negative serial correlations induced by adaptation and the superposition operation of individual processes to create the population activity. Therefore, it suggests that an adaptive ensemble regularizes its collective activity and increases the signal-to-noise ratio and thus it benefits post-synaptic signals detection and/or transmission. Additionally, by applying an information theoretical measures, it is shown that an adaptive process provides more coding capacity due to a regularization of the counting process. This theoretical prediction is confirmed in the superimposed ensemble activity of cortical neurons *in vivo*.

Emergence of sparse code in adaptive network. The other interesting feature of neuronal population with spike-frequency adaptation is that to provide a high-pass filtering of the input fluctuation [Benda 2003]. The high-pass filter affects the transfer function of the neurons and introduces a gain control mechanism. This feature leads to an intensity invariant mechanism, which contributes to the dynamical feature of the neuronal processing [Benda 2007]. In the fourth chapter of this dissertation, the high-pass filtering property of adaptation at the network level is studied. It demonstrates that the high-pass filtering of adaptive neurons in a feed-forward network of neurons can construct a temporally spare representation of the stimulus. In specific, it is shown that adaptation might be responsible for a temporal sparse code which has been reported in the Kenyon cells (KCs) of the insect mushroom body [Turner 2008, Perez-Orive 2002]. The result here provides an alternative understanding to the conventional theory which suggests that the sparse code in Kenyon cells emerges by a feed-forward inhibitory mechanism [Assisi 2007]. Chapter 4 also shows that this theoretical prediction is supported by Calcium imaging experiment that measure activities in Honeybee's mushroom body calyxes. The experimental data indicates that in the presence of the various inhibition antagonist the activity time course of Kenyon cells remains unchanged. Therefore, it suggests that feed-foreword inhibition might not be the sole possible mechanism for the introduction of sparseness. The observed activities in the data alternatively can be explained by the neuronal intrinsic spike-frequency adaptation and/or a similar response impairment mechanisms such as short-term synaptic depression. The result from our simulation of a simplified pathway of the olfactory circuit indicates that implementation of adaptation and/or short-term synaptic depression attributes in the network can account for a sparse representation of the stimulus in Kenyon cell level. Thus, possibly adaptation provides the dynamics to produce a presumably valuable spare code of sensory input in the network. This result can be generalized to many networks in which the machinery for the adaptation is available.

Contributions of this dissertation. Generally, in this dissertation I explore some basic emergent properties of neurons with spike-frequency adaptation on spiking statistics of a single cell, an ensemble activity and finally its possible functional role in an organized network to produce sparse representation of the stimulus e.g. olfactory information processing. Here, I present my theoretical work in parallel to some experimental findings that address the following questions: how does non-renewal statistics affect the variability measures and the coding of the information in spiking neurons *in vivo*? How does a single cell property like spike-frequency adaptation translate to a population level? What are the conditions for the emergence of non-renewal statistics in spiking neurons? How does adaptation contribute to sparse coding strategies?

The results presented here contribute to the understanding of neuronal firings and dynamics by showing that spike-frequency adaptation has a considerable effect on the information processing in the nervous system. Thereby, I strongly suggest that the importance of spike-frequency adaptation and non-renewal statistics should be taken into the account for a better understanding of the functions of spiking neurons in the nervous system.

CHAPTER 2

Serial Correlation in Neural Spike Trains: Experimental Evidence, Stochastic Modelling, and Single Neuron Variability[1]

The activity of spiking neurons is frequently described by renewal point process models that assume the statistical independence and identical distribution of the intervals between action potentials. However, the assumption of independent intervals must be questioned for many different types of neurons. We review experimental studies that reported the feature of a negative serial correlation of neighbouring intervals, commonly observed in neurons in the sensory periphery as well as in central neurons, notably in the mammalian cortex. In our experiments we observed the same short lived negative serial dependence of intervals in the spontaneous activity of mushroom body extrinsic neurons in the honeybee. To model serial interval correlations of arbitrary lags we suggest a family of autoregressive point processes. Its marginal interval distribution is described by the generalized gamma model which includes as special cases the log-normal and the gamma distribution which have been widely used to characterize regular spiking neurons. In numeric simulations we investigated how serial correlation affects the variance of the neural spike count. We show that the experimentally confirmed negative correlation reduces single neuron variability, as quantified by the Fano factor, by up to 50% which favours the transmission of a rate code. We argue that the feature of a negative serial correlation is likely to be common to the class of spike frequency adapting neurons and that it has been largely overlooked in extracellular single unit recordings due to spike sorting errors.

2.1 Introduction

Stochastic point process models have a long tradition in cellular neurophysiology as a means to describe the random nature of action potential generation in spiking neurons [Gerstein 1964, Stein 1965, Moore 1966, Perkel 1967a, Perkel 1967b, Tuckwell 2005, Johnson 1996]. The mathematical definition of a point process allows to analytically calculate the distribution or the expectation value of a given stochastic variable and to formulate statistical predictions for experimental results. Numeric simulation of

[1]This chapter is the reprint version of **Farkhooi, F., Strube-Bloss, M.F. & Nawrot, M.P.** *Serial correlation in neural spike trains: Experimental evidence, stochastic modeling, and single neuron variability.* **Phys. Rev. E 79, 021905 (2009)** available via publisher website at http://link.aps.org/doi/10.1103/PhysRevE.79.021905 . Please refers to page iii in this dissertation for the detials of authors contributions.

point processes is highly efficient and can be used to numerically construct distributions of stochastic variables that are analytically intractable. The class of renewal point processes [Cox 1962] has gained particular popularity in theoretical neuroscience [Stein 1965, Perkel 1967a, Perkel 1967b, Tuckwell 2005, Johnson 1996]. In a renewal model the intervals between successive events are independent and identically distributed. Thus, a renewal process is fully characterized by the distribution of inter event intervals. Selection of the specific model distribution allows to incorporate some important physiological characteristics of spiking neurons such as an absolute and relative refractory period [Tuckwell 2005, Johnson 1996, Berry 1998]. In the intact nervous system spiking neurons modulate their firing rate with time as a means of dynamic stimulus encoding and information processing. Point process models of neuronal spiking that follow a dynamic firing rate can be achieved with inhomogeneous variants of the renewal model where the process intensity follows a deterministic and explicitly time dependent function [Reich 1998, Berry 1998, Kass 2001, Barbieri 2001, Brown 2001, Nawrot 2008, Devroye 1986].

In the renewal model the probability for the occurrence of the ith spike at time t depends solely on the process intensity and the time that elapsed since the last spike $i-1$ at time $T_{i-1} < t$, but there is no serial dependence on the previous history of spiking. However, several types of neurons in different systems have been shown to violate the renewal assumption of independent intervals in their spontaneous activity. The common feature of these neurons is a short-lived negative serial correlation of their inter spike intervals (ISIs) which is likely to be a general property of neurons that feature a physiological mechanism of spike frequency adaptation (see Discussion).

In this manuscript we propose a class of autoregressive point process models that incorporate serial correlation of inter event intervals for arbitrary serial correlation orders. Our model describes the marginal inter event interval distribution by the generalized gamma distribution which includes as special cases the log-normal, the gamma, the exponential and the Weibull distribution. We derive expressions for the most relevant empiric measures of the interval statistics and perform maximum likelihood estimates of the model parameters in our data set. Using physiologically plausible model parameters we investigate the effect of a negative serial correlation on the variability of single neuron discharge.

2.2 Serial interval correlation in different neural systems

The phenomenon of a significant negative serial interval correlation of order 1, i.e. the anti-correlation of neighbouring intervals, is a common property of spiking neurons in various systems. In the sensory periphery this has been observed in the electrosensory P-type receptor of the weakly electric fish [Ratnam 2000, Chacron 2000], sensory ganglion receptors of the paddle fish [Neiman 2004], and in the ganglion cells in the retina of the goldfish [Levine 1980] and of the cat [Kuffler 1957, Rodieck 1967]. In central parts of the mammalian brain the same serial statistics has been reported for brain stem neurons in the lateral superior olive [Tsuchitani 1985], and recently in cortical

Table 2.1: Reports on negative first order serial interval correlation in different preparations and cell types

Ref.	Model System & Neuron Type	SC[2]
[Ratnam 2000]	Weak electric fish, isolated *P*-type Receptors afferent	-0.52
[Chacron 2000]	Weak electric fish, isolated *P*-type Receptors afferent	-0.35
[Neiman 2004]	Paddle fish, sensory Ganglion	$\sim$ -0.4
[Floyd 1982]	Cat splanchnic and hypogastric nerves *in vivo*	-0.3
[Levine 1980]	Goldfish retina, Ganglion cells *in vivo*	-0.13
[Rodieck 1967]	Cat Retina, Ganglion cells *in vivo*	-0.06
[Kuffler 1957]	Cat Retina, Ganglion cells *in vivo*	-0.17
[Tsuchitani 1985]	Cat Lateral Superior Olive *in vivo*	-0.2
[Nawrot 2007]	Rat Somatosensory Cortex (S1) *in vivo*, regular spiking cells	-0.21
[Nawrot 2007]	Rat Somatosensory Cortex (S1) *in vitro*, pyramidal cells	-0.07
[Engel 2008]	Rat medial entorhinal cortex *in vitro* Layer II stellate and Layer III pyramidal neurons	[-0.1,-0.4][3]
Section 2.3	Honeybee central brain *in vivo* Mushroom body extrinsic neurons	-0.15

neurons *in vivo* [Nawrot 2007] and *in vitro* [Nawrot 2007, Engel 2008]. In the present manuscript we report the existence of the same type of short-lived serial dependence of ISIs for a class of central neurons in the mushroom body of the insect brain (cf. 2.3). In Table 2.1 we summarized all quantitative accounts of a negative serial correlation.

2.3 Experimental Results

We investigated serial dependencies of ISIs in the spontaneous activity of extrinsic neurons in the mushroom body (MB) of the honeybee. The mushroom body is known to play a significant role in learning and memory of insects [Menzel 2001]. The extrinsic neurons constitute the readout of the MB and each cell receives converging input from thousands of the MB Kenyon cells, and thereby typically integrates different sensory modalities. Details of the *in vivo* preparation and the extracellular recording technique are described elsewhere [Okada 2007, Strube-Bloss 2008]. In brief, we manufactured extracellular electrodes with three closely spaced polyurethane coated copper wires (14 μm in diameter). The electrodes were inserted into the ventral part of the alpha lobe close to the peduncle, targeting the mushroom body extrinsic neurons, in particular the clusters A1, A2, A4 ,A5, and A7. Raw signals were measured differentially from all three electrode pairs and bandpass filtered at $1 - 9$ kHz using a Lynx-8 amplifier (Neuralynx, Tucson, AZ) before A/D conversion with a sampling frequency of 20 kHz.

Semi-automatic spike sorting was performed to identify the activity of up to three single units using Spike2 software (Cambridge Electronic Design, Cambridge, UK). In order to minimize the inference of potential spike sorting errors with our statistical estimates (see Discussion), we considered for each animal (N=23) only the unit that expressed the highest amplitude of the extracellular spike waveform.

Neural activity was measured under spontaneous conditions, i.e. when the animal was shielded from any sensory stimuli, for up to 20 minutes. Though the experimental condition was controlled, single neuron activity could undergo short episodes with spontaneous modulation of its spike frequency, sometimes in parallel to a spontaneous motor behavior. Such overt changes of the firing rate, however, may severely compromise the statistical analysis of the ISIs [Perkel 1967a]. Thus, in a first step of our analysis we identified in each data set the longest part of stationary activity. To this end, we measured the spike count in successive time bins of a fix length of either 1 s or 500 ms for lower ($< 10\,/\text{s}$) or higher firing rate, respectively, and divided the total series of counts into equal parts of 30 bins. Each subseries of the counting process was then tested for stationarity. We adopt the notion of weak stationarity of a time series [Johnston 1954] which requires three conditions to be fullfilled: The series must have (i) a constant mean, (ii) a finite variance, and (iii) its autocovariance must be translation invariant for an arbitrary time lag. Next, we performed the *Phillips Perron Unit Root Test* (PP test) which is explained in details elsewhere [Phillips 1988]. Briefly, the family of unit root tests estimates the likelihood of a random walk behavior. The random walk is a linear nonstationary time series. The PP test formulates the nullhypothesis: The time series has a unit root, i.e. the time series is *not* stationary. If for a given count series the deviation from nonstationarity was significant ($P < 0.1$) we considered it as stationary. Thereafter, subsequent stationary parts were pooled and the test was repeatedly performed until the longest stationary part was found. We used the *pp.test* function of the *tseries package* in the *R statistical environment* to perform this test. The truncation lag parameter for the linear regression was set to $12(\frac{n}{100})^{0.25}$, suggested by [Trapletti 2011]. Figure 2.1 displays the count series for part of one single neuron recording where black color indicates epochs that were classified as stationary.

From the longest stationary spike train of each neuron we collected all ISIs and estimated their distribution. An example histogram of event intervals is illustrated in Figure 2.2 together with model fits of the log-normal (red) and the centralized gamma distribution (blue, for details on goodness of fit refer to section 2.4). If the spiking process was renewal, an adequate formal model of the ISI distribution would suffice to define the renewal model. However, we found that the assumption of independent intervals was violated in the observed spike train of this neuron. This becomes evident in the conditional mean of ISI length in Figure 2.2 b which estimates for all intervals ISI_i that fall into a given class of interval lengths (bin wifth 15 ms) the average length of the successive intervals ISI_{i+1}.

In general, successive intervals were not independent; in most neurons we observed a tendency for short intervals to be followed by longer ones and vice versa. This dependence was expressed in a negative Spearman rank-order correlation coeffi-

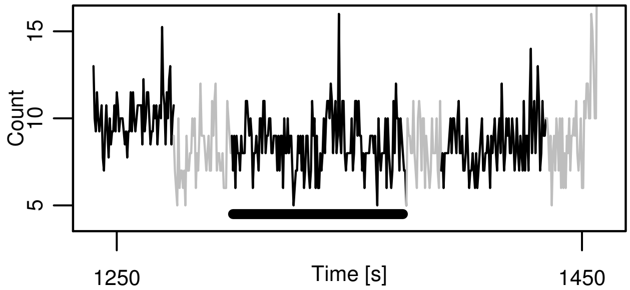

Figure 2.1: Test for weak stationarity of the counting process. Spike count of neuron # 1 observed in successive intervals of 1 s length as a function of time. Gray parts did not deviate significantly from the nullhypothesis of a nonstationary time series. Black parts significantly deviated from this nullhypothesis and were assumed to be weakly stationary. See text for details on the test procedure.

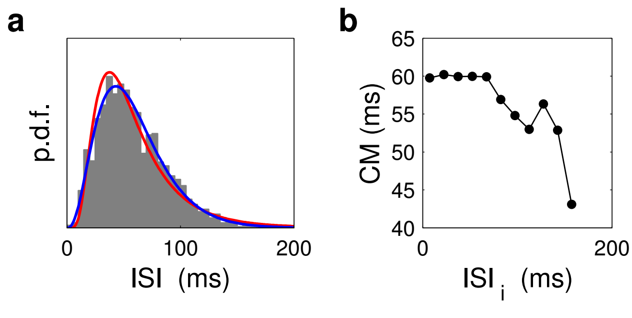

Figure 2.2: Empirical inter spike interval distribution and conditional mean of one MB extrinsic neuron. (a) Histogram of the length of N=1530 ISIs (gray). Log-normal (red) and a gamma (blue) model distribution for MLE parameters. (b) Conditional mean (CM) of the $i+1$st interval in dependence on the length of the ith inteval (estimated in bins of 15 ms).

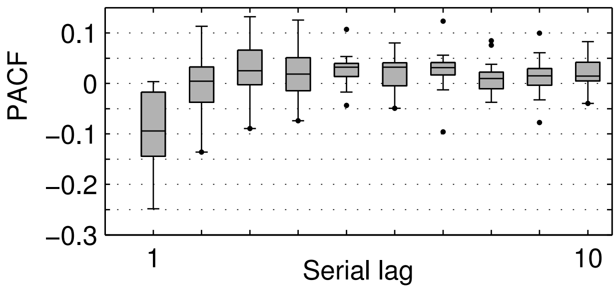

Figure 2.3: Partial autocorrelation function for experimentally observed spike trains. Box plots describe the distribution of rank-order correlation across $N = 21$ neurons for different serial lags. In 14 cases, the sequence of ISIs exhibited a significant ($P < 0.01$) negative correlation of lag 1. For higher lags ($p > 1$) the serial correlation did not significantly deviate from 0 ($P = 0.01$). Here we tested only neurons with a unimodal shape of the interval distribution.

cient [Kendall 1962] of order $p = 1$ (calculated for neighboring intervals). This was found to be significant ($P < 0.01$, Wilcoxon rank-sum test) in 14 out of 21 neurons (Figure 2.3). The example neuron in Fig. 2.2 exhibited a significant serial correlation of -0.05. The average significant correlation coefficient was -0.15.

Next, we tested for significant higher order serial correlation of the intervals I_i and I_{i+p}, separated by lag p. We again used Spearman's rank-order correlation coefficient and estimated the partial autocorrelation function (PACF, [Brockwell 1991]) where for the pth order correlation we use only every pth data sample. This avoids spurious correlation of order p due to correlations of lower orders $l < p$. We found that none of the spike trains exhibited a significant ($P = 0.01$) correlation of higher order $p > 1$ and average correlation coefficients close to zero (Figure 2.3).

2.4 Correlated Point Process model and Parameter Estimation

A linear history dependent process can be modeled by an autoregressive (AR) process within the limits of stationarity and ergodicity conditions (details are elaborated in [Brockwell 1991]). A general form of the autoregressive process with serial dependence up to a finite lag p reads

$$X_s = \beta_1 X_{s-1} + \beta_2 X_{s-2} + ... + \beta_p X_{s-p} + \varepsilon_s \tag{2.1}$$

where ε_s is assumed to be independent and identically distributed with the specific mean μ and finite variance σ^2. β_i is the correlation parameter for the specific lag i.

Under stationary conditions the distribution of X_s is conditional of the distribution of ε_s. Hence, it is possible to generate surrogate sequences with a specific marginal distribution of inter event intervals. As for the renewal model, the choice of the interval distribution is crucial. It determines to a large extend the count and interval statistics of the process. In practical terms, the model distribution should closely resemble the empiric ISI distribution of the particular neuron type that is to be modeled.

2.4.1 Log-normal marginal distribution

In order to modify (2.1) for generating a series of events consistent with our experimental findings, we need to specify (i) the serial correlation structure, and (ii) a marginal interval distribution that describes well our experimental data. With respect to the empirical correlation structure we may simplify the general model (2.1) to consider only the first order serial dependence ($\beta = \beta_1$) which we assume to be negative. As a model for the inter event intervals we chose here the log-normal distribution. This model fits reasonably good to our experimental data (see Fig. 2.2 and Table 2.2) and leads to a rather simple mathematical description. Thus we have

$$\Delta_s = \exp(X_s) = \exp(\beta X_{s-p} + \varepsilon_s) \tag{2.2}$$

where ε_s is assumed to be distributed normally with the mean μ, variance σ^2, and β describes the negative serial dependence of the series X_s. In fact, the series Δ_s of correlated intervals is the exponential transformation of the series of disturbances X_s. The properties of such transformations of correlated random variables is discussed in great detail in [Granger 1976].

The mean and variance of X_s is determined by

$$E[X_s] = \frac{\mu}{1-\beta} \tag{2.3}$$

and

$$Var[X_s] = \frac{\sigma^2}{1-\beta^2} \tag{2.4}$$

respectively. Thereafter, the expected value of Δ_s is

$$E[\Delta_s] = e^{\frac{\mu}{1-\beta} + \frac{\sigma^2}{2(1-\beta^2)}} \tag{2.5}$$

and its variance is

$$Var[\Delta_s] = \left(e^{\frac{2\mu}{1-\beta} + \frac{\sigma^2}{1-\beta^2}}\right) \cdot \left(e^{\frac{\sigma^2}{1-\beta^2}} - 1\right) \tag{2.6}$$

and hence the coefficient of variation of this series is

$$\mathsf{CV}[\Delta_s] = \sqrt{e^{\frac{\sigma^2}{1-\beta^2}} - 1}. \tag{2.7}$$

The intensity λ for this process can be derived directly from (2.5) as

$$\lambda = \frac{1}{E[\Delta_s]} = \frac{1}{e^{\frac{\mu}{1-\beta} + \frac{\sigma^2}{2(1-\beta^2)}}}. \tag{2.8}$$

The autocovariance of Δ_s is given in [Granger 1976], Eq. 2.9.

As we incorporated only first order serial correlation β, by iteration over lags we obtain the following

$$\Delta_s = \exp(X_s) = \exp(\sum_{i=0}^{\infty} \beta^i \varepsilon_{s-i}). \tag{2.9}$$

It is evident that the distribution of Δ_s is conditional on the distribution of ε_s, if the stationary assumption holds ($|\ \beta\ | < 1$). Since the distribution of the ε_s is normal, the distribution of Δ_s is asymptotically log-normal and the series is negatively serially correlated and constitutes a first order Markov process.

Realizations of this autoregressive model are easily obtained by numeric simulation. We performed two example simulations in Figure 2.4 where we defined the log-normal interval distribution by the fix mean interval $E[\Delta] = 50\,\text{ms}$ and a fix coefficient of variation $\mathsf{CV}[\Delta] = 0.5$. The first order serial correlation paramter was either $\beta_1 = -0.1$ (left) or $\beta_1 = -0.5$ (right). Note that by changing β_1 and keeping $E[\Delta]$ and CV fixed, we have to adjust σ and μ according to equations (2.7) and (2.5). The empiric interval distributions in Figure 2.4 a (gray histograms) resemble well the model distributions (red). The return maps of the log-transformed ISIs in Figure 2.4 c disclose the negative correlation of neighbouring intervals and the empiric estimates of the linear correlation coefficient $\hat{\beta}_i$ of log-transformed intervals closely match the underlying model parameters. The empirical PACF for serial correlations of lag $p \geq 2$ are close to zero.

2.4.2 Generalization of the model

We now propose the generalized gamma density as a more general model for the marginal distribution of Δ_s. For $x > 0$ this can be written as

$$\frac{\Omega}{\Gamma(\alpha)}(\frac{1}{\rho})^{\Omega\alpha} x^{\Omega\alpha - 1} e^{-(\rho x)^{\Omega}}. \tag{2.10}$$

This model incorporates some special cases that are widely used to describe experimental ISI distributions of regular spiking neurons. The exponential distribution ($\Omega = \alpha = 1$; e.g. [Gerstein 1964, Perkel 1967a, Tuckwell 2005]) describes the well known special case of a Poisson process with only a single free parameter that determines the mean interval and thus the process intensity. The (centralized) gamma ($\Omega = 1$; e.g. [Kuffler 1957, Stein 1965]), the Weibull distribution, and the log-normal distribution (e.g. [Burns 1976, Levine 1991]) which describes the limiting case for ($\alpha \to \infty$) have one additional free shape parameter.

Following the same scheme as in (2.2) we write

$$\Delta_s = \exp(X_s) = \exp(\beta_p X_{s-p} + \varepsilon_s) \tag{2.11}$$

where ε_s is assumed to be distributed generalized log-gamma with the vector of parameters

$$\zeta = (\rho, \Omega, \alpha)\,. \tag{2.12}$$

Since the distribution of ε_s is log-gamma, the distribution of Δ_s will be asymptotically generalized gamma.

2.4.3 Parameter Maximum Likelihood estimation

The model (2.2) with marginal log-normal distribution has a set of parameters, namely μ, σ and β. To obtain a maximum likelyhood estimator for the paramter set we rewrite the probability density function of the log-normal distribution f_l based on the normal distribution f_N,

$$f_L(\Delta_s;\mu,\beta,\sigma) = \frac{1}{\Delta_s} f_N(\ln\Delta_s;\mu,\beta,\sigma) \tag{2.13}$$

Thus, we can write the log-likelihood function of the log-normal distribution (l_L) as

$$\begin{aligned} l_L(\mu,\beta,\sigma \quad & \mid \Delta_1,\Delta_2,\dots\Delta_n) = \\ & -\sum_k \ln\Delta_k \\ + \quad & l_N(\mu,\beta,\sigma \mid \ln\Delta_1,\ln\Delta_2,\dots\ln\Delta_n) \end{aligned} \tag{2.14}$$

Since $\sum_k \ln\Delta_k$ is constant with regard to μ, σ and β, both logarithmic likelihood functions, l_L and l_N, reach their maximum with the same μ, β and σ. Hence, using the expression for the maximum likelihood estimators (MLE) for the normal distribution we can deduce the MLE for the parameters of the log-normal distribution [Johnston 1954]. MLEs for the generalized gamma model are given in [Ortega 2003]. Using the lemma (2.14) we may obtain the MLEs for the generalized log-gamma distribution. In practical terms, when estimating parameters from a sample $\{\hat{\Delta}\}$ of experimentally obtained intervals we may first perform a logarithmic transformation and then apply the MLE estimators on the transformed sample $\{\log(\hat{\Delta})\}$.

Maximum likelihood estimation ensures a bias-free parameter estimation with minimal variance of the estimator. Applying non-optimal estimators will lead to a biased estimate. The linear correlation coefficient assumes a normal distribution of the random variable and will introduce a bias for log-normal distributed random variables. We illustrate this in Figure 2.5 where we simulated realizations of the model described in (2.2) and subsequently obtained two different estimates $\hat{\beta}$ of the serial interval correlation parameter β. The red circles in Figure 2.5 indicate the estimated values obtained by MLE on the ordinate which closely match the true parameter values on the abscissa. However, the linear serial correlation coefficient (black circles) strongly underestimates the model-inherent serial correlation β with an increasing estimation error for increasing absolute values of β.

2.4.4 Empiric estimates of model parameters

In practice, we rarely know for certain that a sample of observed event intervals are drawn from a specific distribution. Instead, the best we can typically do is to provide evidence that our observations are consistent with a distribution model. A goodness-of-fit test can be performed to assess whether the observations were likely to be drawn from the hypothesized model distribution which is particularly helpful when choosing between alternative models. We used the Kolmogorov-Smirnov test to assess the goodness of fit of the log-normal and the centralized gamma distribution to the empiric ISI distribution for 10 different neurons. In order to perform the test correctly, distribution model parameters were estimated based on the assumed distribution using maximum likelihood estimators (MLE). The test results for 10 example units are illustrated in Table 2.2. In summery, the test indicates that the model cannot be rejected in approx. 75% and 50% of all neurons for the log-normal and the centralized gamma distribution, respectively ($P \leq 0.01$). Moreover, all units were tested for unimodality based on a test suggested in [Hartigan 1985]. Only two neurons showed a significant deviation of their ISI distribtion from unimodality (neurons #5 and #7 in Table 2.2).

Table 2.2: Estimated parameters from experimental spike trains of 10 neurons for the autoregressive log-normal and centralized gamma model with 1st order serial correlation $\hat{\beta}$. Neurons 5 and 7 showed a significant (P=0.05) deviation from a unimodal distribution.

	Log-normal				Centralized Gamma				
#	$\hat{\mu}$	$\hat{\sigma}$	**P**[1]	$\hat{\beta}$	$\hat{\alpha}$	$\hat{\rho}$	**P**[1]	$\hat{\beta}$	CV
01	-3.245	1.361	0.090	-0.006	0.797	0.103	0.339	-0.006	1.24
02	-2.239	0.545	**0.000**	-0.268	4.291	0.028	**0.000**	-0.268	0.66
03	-4.628	0.875	**0.011**	0.018	1.581	0.009	**0.028**	0.018	0.88
04	-3.057	0.721	**0.000**	-0.189	2.409	0.024	**0.013**	-0.190	0.61
05	-1.521	1.048	0.759	-0.424	1.129	0.321	0.238	-0.442	0.96
06	-4.232	1.002	**0.000**	-0.103	1.303	0.017	**0.000**	-0.103	0.86
07	-2.974	0.555	**0.013**	-0.062	3.762	0.016	0.477	-0.062	0.51
08	-3.088	1.132	**0.000**	-0.215	1.047	0.075	**0.000**	-0.216	0.96
09	-2.955	0.568	**0.049**	0.007	3.695	0.016	0.780	0.007	0.51
10	-4.077	1.045	**0.013**	-0.068	1.226	0.022	0.222	-0.068	1.06

2.5 Effect of serial interval correlation on count variability

Stochastic point processes are typically described by two inherent stochastic variables. These are the intervals Δ between events, and the event count N_T, i.e. the number of events that are expected to fall within a certain time interval of length T. For any given point process, interval and count statistics are closely related. We investigated the effect of serial interval statistics on the variability of the event count in numerical simulations of our model (2.2). To quantify the count variability we used the Fano factor [Fano 1947, Nawrot 2008] (also 'index of dispersion') which normalizes the count variance by the mean count across observations of length T:

$$\mathsf{FF} = \frac{Var[N_T]}{E[N_T]}.$$

For renewal models the count variability depends solely on the dispersion of the interval distribution and it holds in the limit of infinite observation that $\lim_{T\to\infty} \mathsf{FF} = \mathsf{CV}^2$ ([Cox 1962, Cox 1966, Tuckwell 2005]). This relation will change if the inter event intervals are no longer independent but exhibit serial dependencies. Cox & Lewis 1966 ([Cox 1966]) derived the following approximate analytic expression for the effect of serial interval correlation of order p on a point process that is otherwise stationary

$$\lim_{T\to\infty} \mathrm{FF} = \mathsf{CV}^2_{\mathrm{th}}\Big[1 + 2\sum_{p=1}^{\infty}\beta_p\Big]. \tag{2.15}$$

Using our model (2.2) we explored the FF as a function of first order serial interval correlation β in numeric simulations. We again fixed the parameters of mean interval μ and the CV. For each parameter value of β we then generated 10000 point process realisations and computed the FF across all repetitions. Our results in Figure 2.6 a show that the FF increases with increasing values of *positive* serial correlation, while it decreases with increasing strength of *negative* correlation. In Figure 2.6 b we directly explored the ratio $\mathsf{FF}\,/\,\mathsf{CV}^2$. It emphasizes the effect of serial correlation on count variability in comparison to the renewal case for which $\mathsf{FF} \approx \mathsf{CV}^2$. The linear expression (2.15) approximates the numeric result only in a restricted paramter range with $\beta \approx 0$. We conclude that the process (2.2) with a realistic negative correlation strength in the experimentally observed range of $\beta \in [-0.5, -0.1]$ (cf. Table 2.1) exhibits a count variance that is up to 50 % *smaller* than predicted from the renewal model.

2.6 Discussion

We report here a negative first order serial correlation of ISIs in the spontaneous activity of mushroom body extrinsic neurons in the honeybee. The estimated negative correlation was generally weak but significant in the majority of units. Short-lived serial interval correlations have been previously observed in the spontaneous activity of various different types of neurons and with different correlation strengths up to approx. -0.5 for neighboring intervals, as summarized in Table 2.1. This indicates that the spiking processes of those neuron types generally exhibit a non-trivial dependence on the spiking history. In other words, the dynamics underlying a neuron's spike generation is not reset after each spike as it is assumed in the prominent renewal model as well as in many computational single neuron models.

2.6.1 The effect of spike sorting errors

Why are there so few reports on the negative interval correlation in the activity of single neurons in central brain structures (cf. Table 2.1)? Potential errors during the procedure of spike sorting in extracellular recordings may lead to the false assignment of individual spikes to one single unit (false positive spikes), or to missed spikes of one neuron (false negative spikes). Both types of errors will reduce the strength and significance of the empircial correlation measure (simulations not shown). In paractice, spike sorting errors are inevitable and abundant. E.g. the rate of false positive assignment has been estimated to reach $\approx 10\,\%$ in the neocortex and a similar number of spikes of a particular neuron are likely to be missed (e.g. [Joshua 2007, Pouzat 2004]). This can readily explain why the phenomenon of serial interval correlation has been largely overlooked in *in vivo* preparations where single neuron activity is accessible mainly through extracellular recording techniques, in particular in the awake animal. Conversely, if we assume that neurons of a certain class do exhibit a particular serial correlation pattern we might be able to exploit this knowledge in the context of a spike sorting procedure. In particular we suggest here to use the significance of the observed 1st order negative serial correlation of a putative single unit as a post-hoc quality measure for the success of the spike sorting algorithm. This will require the continuous measurement of stationary spontaneous activity during parts of the experiment.

2.6.2 The cause of negative serial interval correlation

The feature of negatively correlated intervals is likely to be a neuron intrinsic property caused by the same cellular mechanisms that underlie spike frequency adaptation (SFA). The combinatorial effect of calcium influx associated with action potential generation, slow decaying intracellular calcium dynamics and a calcium dependent potassium current mediates the so-called slow afterhyperpolarization (e.g. [Pennefather 1985, McCormick 1989, Sanchez-Vives 2000a, Tzingounis 2007, Wang 1998, Liu 2001]). In the spontaneous state this adapting mechanism may lead to an alteration of short and long intervals. Conversely, significant anti-correlation of neighboring intervals in experimental spike trains is indicative of SFA [Liu 2001] and measures of negative serial correlation may be applied to actually collect evidence for SFA in recordings from awake animals. However, one cannot exclude the possibility that the statistics of the synaptic input under spontaneous conditions causes or alters the serial statistics of the output spike train. For example in the primary afferent neurons of the electrosensors in the paddle fish serial correlation of alternating sign exist up to very high serial orders [Neiman 2001, Neiman 2004, Neiman 2005]. This is due to an oscillatory input from hair cells that couples to a second neuron intrinsic oscillator. In an aged preparation where the primary afferent is devoid of its input and thus decoupled from the afferent oscillation, higher order correlations rapidly decay except for the strong negative 1st order correlation which is caused by neuron intrinsic properties [Neiman 2005].

2.6.3 Computational Models

We briefly discuss existing models at different levels of abstraction that have been shown to reproduce the experimentally observed negative serial correlation. The choice of a model at the appropriate level of complexity obviously depends on the specific questions under study [Herz 2006]. Zacksenhouse et. al. [Zacksenhouse 1998] devised a compartmental model of the principal cells of the mammalian lateral superior olive (LSO). Only the inclusion of Ca^{2+} dependent K^{+} channels could reproduce a negative serial dependence of neighboring ISIs that resembled those observed in *in vivo* single unit recordings from the LSO of the anesthetized cat [Tsuchitani 1985]. In the same issue, Wang [Wang 1998] presented a biophysical model of a cortical pyramidal neuron with one single dendritic and a somatic compartment. Incorporation of a voltage gated

Ca^{2+} conductance and a Ca^{2+} dependent K^+ conductance produced a pronounced SFA behavior and negative serial correlation of successive intervals for stationary input conditions. The model predicted that the strength of the negative correlation increases with the output firing rate. This has recently been confirmed in an experimental *in vitro* preparation [Engel 2008] and quantitative prediction for the average correlation coefficient of -0.3 was well met by the recent experimental estimates listed in Table 2.1.

Using a generalized leaky integrate and fire (I&F) model with spike frequency adaptation, Liu and Wang [Liu 2001] predicted values for negative serial interval correlations in cortical pyramidal neurons, again in the range of -0.19 to -0.24. Recently, Müller et al. [Muller 2007] presented a conductance based I&F model with SFA. The neuron, when driven by excitatory and inhibitory synaptic input, reproduces negative serial interval correlation, the strength of which is rate dependent. This model can be reduced to a Markov process for spike frequency adapting neural ensembles by adiabatic elimination of fast variables [Muller 2007]. This elegant approach synthesizes existing mean adaptation approaches, population density methods, and inhomogeneous renewal theory, resulting in a unified and tractable framework which goes beyond renewal and mean-adaptation theories by accounting for correlations between subsequent inter spike intervals.

At the next level of reduced complexity, the classic I&F model has been modified to produce negative interval correlations by numerical simulation. Introducing a dynamic fatigue of the spike threshold that decays exponentially with physical time introduces a threshold memory [Chacron 2000, Chacron 2001, Brandman 2002, Longtin 2003, Lüdtke 2006]. The maximal order and strength of significant serial correlations is then rate dependent. A simpler modification of the I&F model [Chacron 2004] assumes a threshold memory of fix serial order k and thus produces negative serial correlations only up to order k, independent of the rate.

2.6.4 Point Process Models

Point processes represent a different category of abstract models. They do not provide a complete model of the single neuron as an input-output system. In the mathematical definition, the point process intensity is a predescribed deterministic or stochastic function that describes the time dependence of the event rate, i.e. of the neuron's *output*. Synaptic input per se does not find its analogon in these models. However, so-called cascade models (cf. [Herz 2006]) combine an input stage that converts synaptic drive into an intensity variable with a random point process that genereates the spike output. The merits of a stochastic point process model is its analytic formulation and a highly efficient numeric simulation.

We presented a simple autoregressive (AR) point process model that may be seen as a straight foreword extension of the widely used renewal model and earlier interval models with serial dependencies [Wold 1954, Gaver 1980]. Our approach models a linear AR process that draws random disturbances ε where the distribution of the random variable ε is represented on log scale (e.g. the log-gamma distribution). We then exponentially transform the resulting sequence to obtain the final sequence of non-negative intervals (e.g. gamma model). The experimentally observed single unit spike trains showed in all but two cases an unimodal interval distribution that in many cases could be well fitted by a log-normal or centralized gamma distribution (cf. Table 2.2). Our model can be generalized for any well defined interval distribution [Kampen 2007]. The linear serial correlation coefficients up to finite lag p directly enter our model (2.2). Empiric estimates of the parameters β_i are obtained using appropriate ML estimators based on a concrete model distribution. An alternative model-free and reliable estimator is provided by Spearman's rank-order correlation coefficient ([Kendall 1962, Press 1992], cf. Figure. 2.3) which replaces the real valued intervals by their rank among all intervals which are assumed to be uniformly distributed. Its disadvantage in comparison to the appropriate ML estimator is expressed in the reduced power of the significance test [Lehmann 1953]. For our model we apply the PACF to estimate the serial correlation parameters. This requires a sample size that increases only linearly with serial correlation order p and allows for parameter estimation from realistic experimental sample sizes.

A more general approach for generating history dependent sequence of intervals rests on the conditional probability density function of an interval given the lengths of the previous intervals as it is described in [Johnson 1996]. This approach of formulating a point process model with serial correlations up to a lag p requires a model of the full p-dimensional interval distribution, or likewise the p-dimensional hazard term. The difficulty of this approach obviously lies in the empiric estimate of the distribution parameters from experimental data. The number of intervals that is required for a faithful estimate will generally increase exponentially with the power of $(p + 1)$.

The formulation of the conditional intensity function [Vere-Jones 2005] provides a rather general framework to relate the intensity of a point process to its event history and other covariate functions such as the intensity and spiking history of parallel processes [Truccolo 2005]. However, empiric estimation of the conditional intensity function typically requires a large amount of experimental data.

2.6.5 Reduced single neuron discharge variability

The variability of the single neuron discharge across repeated observations, as quantified by the FF, has been extensively studied in various experimental systems. It may be interpreted as noise with respect to the signal encoded in the single neuron's firing rate which is implicitely assumed to be identical in all experimental repetitions. In point process theory interval and count statistics are directly related. In the renewal case the variance of the interval distribution fully determines the variance of the spike count. Numeric simulations of our non-renewal model predict that the variability of single neuron discharge is smaller than expected under the renewal assumption for all neurons that show the typical feature of a negative serial interval correlation in their spontaneous activity. The very same prediction has previously been established by Chacron et al. [Chacron 2004] in numeric simulatios of their integrate & fire model with dynamic threshold. Experimental findings confirm this model prediction. Under spontaneous conditions the P-type recptor of the weakly electric fish produce regular spike trains with a strong 1st order negative serial correlation [Ratnam 2000, Chacron 2000]. This resulted in a Fano factor that was much smaller than predicted under the renewal assumption, i.e. for a random permutation of the empiric interval series [Chacron 2000]. We could show elsewhere [Nawrot 2007] that cortical spike trains *in vivo* exhibited a negative serial interval correlation with an average strength of $\hat{\beta}_1 \approx -0.2$. This lead to a FF that was about 30% smaller than the CV^2 which matches well our numerical calibration in Figure 2.6. The effect of a reduced count variability is naturally also expressed in the spectral analysis of a spike train. Under stationary conditions, the negative serial correlation reduces the power of the noise spectrum at low frequencies [Chacron 2004, Neiman 2004] which enhances the information transfer in the low frequency domain [Chacron 2004]. Note that this effect diminishes at high frequencies. This frequency dependence is equally expressed in the dependence of the FF on the lenght T of the observation interval. For shorter intervals the FF tends to unity $\lim_{T\to 0} \mathsf{FF}(T) = 1$, while the CV tends to zero, independent of the stochastic nature of the underlying process [Nawrot 2008].

As discussed above, we must expect that erronous spike sorting has frequently lead to the analysis of 'single unit activity' that was not 100 % single neuron activity If we assume a negative interval correlation in the single neuron activity, we may deduce two major effects of spike sorting erors on the statistics of the sorted unit activity: (1) The FF increases when serial correlation diminishes, and (2) the variance of the interval length (CV) likely increases due to false positive and false negative spikes that truncate or merge the original spike trains with a biased production of too short and too long intervals. We may speculate that spike sorting errors may have lead to a systematic overestimation of count and interval variability, and thus may have caused a biased picture of single neuron variability. We believe that a cautious re-evaluation of serial spike train statistics, and of spike count variability is necessary, particularly in the *in vivo* activity of central neurons. As we have discussed elsewhere [Nawrot 2008], additional factors may lead to an overestimation of the true single neuron variability in experimental recordings from awake animals. In central brain structures the most prominent influence is to be expected from ongoing activity that is not directly related to the experimental task under observation [Arieli 1996, Leopold 2003, Nawrot 2003, Rotter 2005].

As outlined above, we hypothesize that the large class of neurons that feature an intrinsic SFA mechanism generally exhibit a negative serial correlation under spontaneous conditions. We may thus formulate the futher going hypothesis that the SFA mechanism reduces count variability not only under spontaneous conditions, but generally also under response conditions. This would result in a more reliable transmission of a signal in favor of a rate code [Farkhooi 2008]. Lüdtke et al. (2006) demonstrated in a model study that postsynaptic neurons can directly exploit the non-renewal structure of a presynaptic spike train and benefit from an enhanced sensitivity to weak signals on a noisy background [Lüdtke 2006].

2.6.6 Open source tools

We provide implementations of various tools for numeric point process simulation and parameter estimation within the FIND open source toolbox for neural data analysis with Matlab [Meier 2008] (http://find.bccn.uni-freiburg.de/). Implementations in Python will be made available at the portal site of G-Node [Herz 2008] (www.neuroinf.de), the German node of the International Neuroinformatics Coordinating Facilites (INCF).

2.7 Acknowledgments

We are grateful to Eilif Muller, Stefan Rotter, Benjamin Staude and Randolf Menzel for fruitful discussions. We thank Clemens Boucsein for making available the rat cortical data for reanalysis in Figure 2.6. This research is supported by the Federal Ministry of Education and Research (BMBF), grant 01GQ0413 to BCCN Berlin.

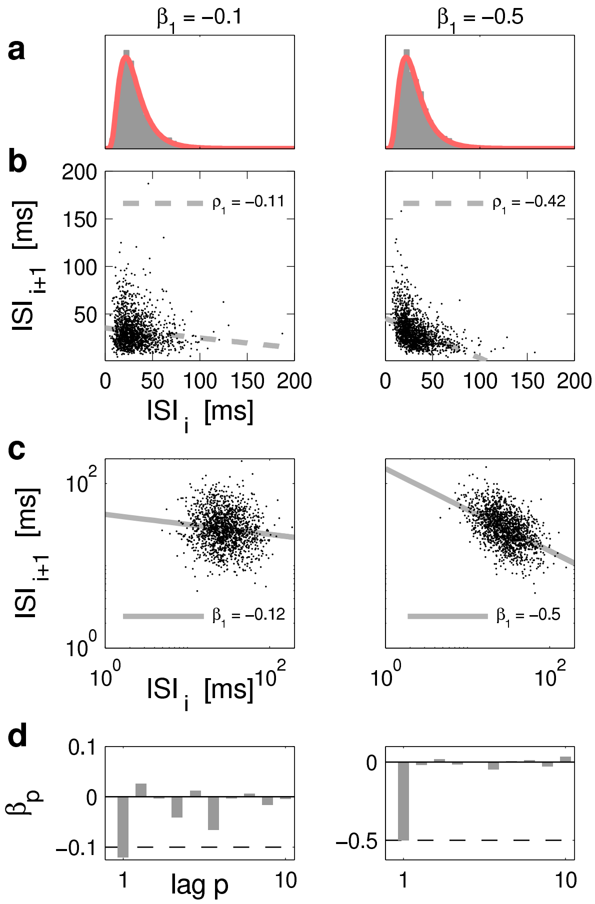

Figure 2.4: Numeric simulations of the log-normal model. The parameter of first order serial correlation was set to either $\beta_1 = -0.1$ (left) or $\beta_1 = -0.5$ (right). The parameters of $E[\Delta] = 50ms$ and CV $= 0.5$ were fixed for both cases. (a) Model (red) and empiric (gray) interval distribtion show a good agreement. (b) Interval return map. The serial dependence of the $i + 1st$ on the ith interval is difficult to see. The linear regression (dashed line) with linear correlation coefficient ϱ_1 of the interval series Δ_s underestimates the correlation parameter β_1. (c) In the interval return map of the log-transformed series $\log(\Delta_s)$ the strong negative correlation is clearly visible (right). The empiric correlation coefficient $\hat{\beta}_1$ is an unbiased estimate of the true correlation β_1. (d) PACF estimated for serial lags $p \leq 10$.

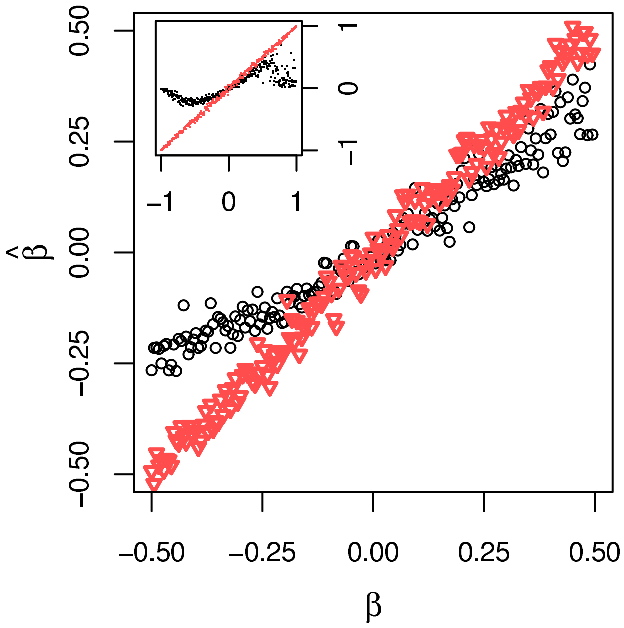

Figure 2.5: Comparison of linear correlation coefficient (black) and MLE estimator for $\hat{\beta}$ (red). Each single estimate is based on a numeric simulation of 10.000 intevals with parameters of neuron # 1 in Table 2.2. The serial correlation paramter β has been varied in the range [-0.99, 0.99].

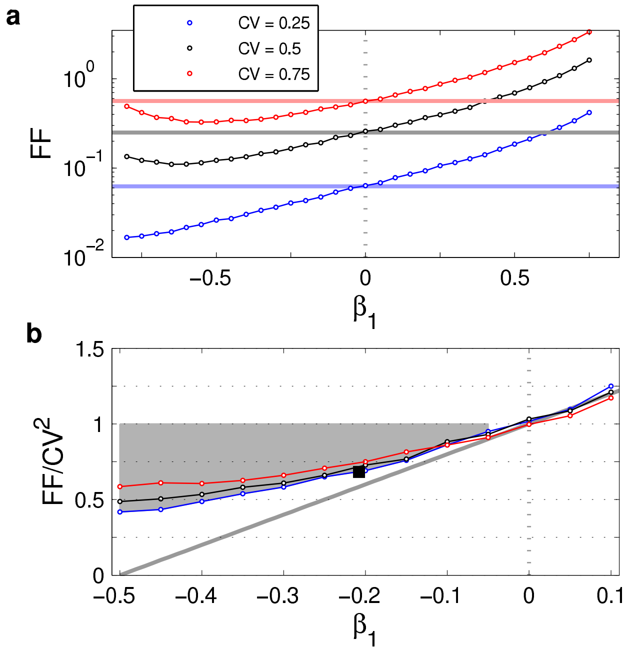

Figure 2.6: Effect of serial interval correlation on spike count variability. We obtained numerical spike train realizations using our model (2.2). We varied the serial correlation paramter β and adjusted the parameters (μ, σ) to obtain a fixed value of CV. (a) Fano factor (FF) as a function of β for three different values of CV as indicated. The horizontal lines indicate the expectation $\mathsf{FF} = \mathsf{CV}^2$ for a renewal process. The vertical dotted line represents the renewal model where $\beta = 0$. (b) Ratio of FF and CV^2. For the physiologically relevant range with negative 1st order serial correlation $\beta \in [-0.5, -0.1]$ (cf. Table 2.1) the FF is clearly smaller than the CV^2 (gray shaded area). For the renewal model ($\beta_1 = 0$) we find $\mathsf{FF} / \mathsf{CV}^2 \approx 1$ as expected. The gray line represents the linear approximation (2.15). Each data point represents 10000 trials. Each trial comprised on average 100 spikes; this number is sufficiently large to avoid a significant bias of estimation for FF and CV^2 [Nawrot 2008]. The black square reproduces the results given in [Nawrot 2007] as the average for 7 cortical neurons with significant 1st order serial correlation of ISIs (see Discussion).

Chapter 3

Adaptation Reduces Variability of the Neuronal Population Code[1]

Sequences of events in noise-driven excitable systems with slow variables often show serial correlations among their intervals of events. Here, we employ a master equation for general non-renewal processes to calculate the interval and count statistics of superimposed processes governed by a slow adaptation variable. For an ensemble of spike-frequency adapting neurons this results in the regularization of the population activity and an enhanced post-synaptic signal decoding. We confirm our theoretical results in a population of cortical neurons.

3.1 Introduction

Statistical models of events assuming the renewal property, that the instantaneous probability for the occurrence of an event depends uniquely on the time since the last event, enjoys a long history of interest and applications in physics. However, many event processes in nature violate the renewal property. For instance, it is known that photon emission in multilevel quantum systems constitutes a non-renewal process [Soler 2008]. Likewise, the time series of earthquakes typically exhibits a memory of previous shocks [Livina 2005], as do the times of activated escape from a metastable state, as encountered in various scientific fields such as chemical, biological, and solid state physics [Lindner 2007]. Often, the departure from the renewal property arises when the process under study is modulated by some slow variable, which results in serial correlations among the intervals between successive events. In particular, the majority of spiking neurons in the nervous systems of different species show a serial dependence between inter-event intervals (ISI) due to the fact that their spiking activity is modulated by an intrinsic slow variable of self-inhibition, a phenomenon known as spike-frequency adaptation [Liu 2001, Farkhooi 2009b].

In this letter, we present a non-renewal formalism based on a population density treatment that enables us to quantitatively study ensemble processes augmented with a slow noise variable. We formally derive general expressions for the higher-order interval and count statistics of single and superimposed non-renewal processes for arbitrary observation times. In spiking neurons, intrinsic mechanisms of adaptation reduce output variability and facilitate population coding in neural ensembles. We confirm our

[1] The material in this chapter is a preprint of **Farkhooi, F., Muller, E. & Nawrot, M.P.** *Serial correlation in neural spike trains: Experimental evidence, stochastic modeling, and single neuron variability.* **Phys. Rev. E 83, 050905 (2011)** and its final version available in the publisher website via http://link.aps.org/doi/10.1103/PhysRevE.83.050905. This version assessable via ArXiv at http://arxiv.org/abs/1007.3490v2. Please refers to page iii in this dissertation for the detials of authors contributions.

theoretical results in a set of experimental *in vivo* recordings and analyse their implications for the read-out properties of a postsynaptic neural decoder.

3.2 Non-renewal Master Equation

We define the limiting probability density for an event given the state variable x by the so-called hazard function $h_x(x,t)$ where t denotes explicit dependence on time due to external input following [Muller 2007] and appendix A. Here, we assume x has a shot-noise-like dynamics, which is widely used as a model of spike induced neuronal adaptation [Muller 2007]

$$\dot{x} := -x(t)/\tau + q\sum_k \delta(t-t_k), \tag{3.1}$$

where δ is the Dirac delta function, t_k is the time of the k^{th} event, and q is the quantile change in x at each event. The dynamics of x deviates from standard treatments of shot-noise (such as in [Gardiner 2004]) in that the rate of events has a dependence on x as expressed by the hazard function $h_x(x,t)$. It is straightforward to show that the distribution of x in an ensemble, denoted by $\Pr(x,t)$, is governed by

$$\begin{aligned}\partial_t \Pr(x,t) &= \partial_x[\frac{x}{\tau}\Pr(x,t)] + h_x(x-q,t)\Pr(x-q,t) \\ &- h_x(x,t)\Pr(x,t). \end{aligned}\tag{3.2}$$

Much insight can be gained by applying the method of characteristics [de Kamps 2003] to establish a link between the state variable x and its time-like variable t_x. For Eq. (3.1) we define $t_x = \eta(x) := -\tau\ln(x/q)$, whereby $\frac{d}{dt}t_x = 1$. When an event occurs, $t_x \mapsto \psi(t_x)$, where $\psi(t_x) = \eta(\eta^{-1}(t_x)+q) = -\tau\ln(e^{-t_x/\tau}+1)$ with its inverse given by $\psi(t_x)^{-1} = -\tau\ln(e^{-t_x/\tau}-1)$. Thus, we define $h(t_x,t) := h_x(\eta^{-1}(t_x),t)$. This transformation of variables to t_x elucidates the connection of the model to renewal theory. Here, the reset condition after each event is not $t_x \mapsto 0$ (renewal) but $t_x \mapsto \eta(x+q)$, for details refer to appendix A. Therefore, the variable t_x that we may call a 'pseudo age' is a general state variable that no longer represents the time since the last event (age). Transforming variables in Eq. (3.2) from x to t_x yields in the steady state

$$\begin{aligned}\partial_{t_x}\Pr(t_x) &= -h(t_x)\Pr(t_x) \\ &+ (1-\Theta_0(t_x))[h(\psi^{-1}(t_x)\Pr(\psi^{-1}(t_x))], \end{aligned}\tag{3.3}$$

where $\Theta_0(t_x)$ is the Heaviside step function, and for convenience we defined $\psi^{-1}(t_x \geq 0) \equiv 0$. An efficient algorithm for solving Eq. (3.3) is given in [Muller 2007]. We denote this solution by $\Pr_{eq}(t_x)$. Further, the time-like transformation in Eq. (3.3) allows computation of the ISI by analogy to the renewal theory [Muller 2007] and also permits the comparison to the master equation for a renewal process as given in Eq. (6.43) in [Gerstner 2002]. The distribution of t_x just prior to an event is a quantity of interest and it is derived as $\Pr^*(t_x) = h(t_x)\Pr_{eq}(t_x)/r_{eq}$, where $r_{eq} = \int h(t_x)\Pr_{eq}(t_x)dt_x$ is a normalizing constant and also the process intensity or rate of the ensemble. Similarly, one can derive the distribution of t_x just after the event, $\mathrm{Pr}^{\dagger}(t_x) = \mathrm{Pr}^{*}(\psi^{-1}(t_x))\frac{d}{dt_x}\psi^{-1}(t_x)$ [Muller 2007]. Then the relationship between t_x and the ordinary ISI distribution can be written as

$$\rho(\Delta) = \int_{-\infty}^{+\infty} h(t_x+\Delta)\Omega(t_x+\Delta)\mathrm{Pr}^{\dagger}(t_x)dt_x, \tag{3.4}$$

where $\Omega(t_x+\Delta) = e^{-\int_{t_x}^{\Delta} h(t_x+u)du}$. Now the n^{th} moment μ_n of the distribution and its coefficient of variation C_v can be numerically determined.

3.3 Counting Statistics

In order to derive the count distribution, we generalize the elegant approach for deriving the moment generating function as introduced in [van Vreeswijk 2010]: let $\rho_n(t_n, t_x^n|t_x^0)$ be the joint probability density given its initial state t_x^0, where t_n stands for time to n^{th} event and t_x^n is the corresponding adaptive state of the process. Thereafter, one can recursively derive

$$\tilde{\rho}_{n+1}(s, t_x^{n+1}|t_x^0) = \int \tilde{\rho}_n(s, t_x^n|t_x^0)\tilde{\rho}(s, t_x^{n+1}|t_x^n)dt_x^n, \tag{3.5}$$

where $\tilde{\rho}_{n+1}(s, t_x^{n+1}|t_x^0) = \mathcal{L}[\rho_{n+1}(t_{n+1}, t_x^{n+1}|t_x^0)]$ and $\mathcal{L}$ is the Laplace transform with resepect to time, assuming $\tilde{\rho}_1(s, t_x^1|t_x^0) = \tilde{\rho}(s, t_x^1|t_x^0)$ [van Vreeswijk 2010]. Next, defining the operator $\mathbf{P}_n(s)$ and applying bra-ket notation as suggested in [van Vreeswijk 2010], leads to the Laplace transform of n^{th} events ordinary density

$$\tilde{\rho}_n(s) = \langle 1 \mid \mathbf{P}_n(s) \mid \mathrm{Pr}^{\dagger}\rangle = \langle 1 \mid [\mathbf{P}(s)]^n \mid \mathrm{Pr}^{\dagger}\rangle, \tag{3.6}$$

where the operator $\mathbf{P}$ associated with $\tilde{\rho}(s)$, which interestingly corresponds to the moment generating function of the sum of n non-independent intervals $\tilde{f}_n(s)$ as defined in [McFadden 1962]. Now, following Eqs. (2.15) in [McFadden 1962] Laplace transform of count distribution denoted as $\tilde{P}(n, s)$.

The Fano factor provides an index for the quantification of the count variability. It is defined as $J_T = \sigma_T^2/\mu_T$, where σ_T^2 and μ_T are the variance and the mean of the number of events in a certain time window T. It follows from the additive property of the expectation that $\mu_T = \int_0^T r(u)du$ and assuming constant firing rate $\mu_T = r_{eq}T$. To calculate the second moment of $\tilde{P}(n, s)$, we require $\tilde{\mathcal{A}}_s = \sum_k \tilde{\rho}_k(s)$, thus

$$\tilde{\mathcal{A}}_s = \langle 1 \mid \mathbf{P}(s)(\mathbf{I} - \mathbf{P}(s))^{-1} \mid \mathrm{Pr}^{\dagger}\rangle, \tag{3.7}$$

where $\mathbf{I}$ is the identity operator. Note, assuming a renewal interval distribution in Eq. (3.4) one obtains $\tilde{\mathcal{A}}_s^r = \tilde{\rho}(s)/(1-\tilde{\rho}(s))$ and $\mathcal{L}^{-1}[r_{eq}\tilde{\mathcal{A}}_s] = r_{eq}\mathcal{A}(u)$ is the joint density of an event at time t and another event at time $t+u$. Thus, the autocorrlation of events is $A(u) = r_{eq}[\delta(u) + \mathcal{A}(u)]$. Now, by using Eq. (3.7) and the Eq. (3.3) in [McFadden 1962], the second moment of the count statistics can be derived. Thus, we obtain the Fano factor

$$J_T = 1 + (2/T)\int_0^T (T-u)\mathcal{A}(u)du - r_{eq}T, \tag{3.8}$$

The asymptotic property of $F = \lim_{T\to\infty} J_T$ can be derived from the result stated in Eq. (7.8) in [McFadden 1962] as

$$\lim_{s\to 0}[\tilde{\mathcal{A}}_s - 1/(\mu_1 s)] = C_v^2[1/2 + \sum_{k=1}^{\infty} \xi_k] - 1/2, \tag{3.9}$$

where ξ_k is the linear correlation coefficient between two k lagged intervals. Provided the limit exits, we find $F = C_v^2[1 + 2\sum_{k=1}^{\infty} \xi_k]$ in [Cox 1966].

3.4 Superposition

We now generalize our results on the counting statistics to the superposition of independent point processes. This is of practical interest in all cases where we observe superimposed events that stem from multiple independent process, e.g. in photon detection devices, or in the case of a postsynaptic neuron that receives converging inputs from multiple lines. We study the superposition of k stationary, orderly, and independent processes. The ensemble process will have a rate $\check{r} = \sum_{i=1}^{k} r_i$ and following Eq. (4.18) in [Cox 1980] $\check{\mathcal{A}}(u) = \check{r} + \check{r}^{-1}\sum_{i=1}^{k} r_i[\mathcal{A}_i(u) - r_i]$. Here, for the sake of simplicity, we derive the desired relationship between C_v^2 and the ensemble $\check{F}$ for k identical processes. To this end, we plug $\check{r}$ and $\mathcal{L}[\check{\mathcal{A}}(u)]$ into the Eq. (3.9) and therefore it becomes $\lim_{s\to 0}[\tilde{\mathcal{A}}_s - 1/(\mu_1 s)] = \mathsf{CV}^2[1/2 + \Xi] - 1/2$, where CV and $\Xi = \sum_{i=1}^{\infty} \Xi_i$ are the coefficient of variation and the interval correlations of the superimposed process. Note that the left hand side of this equation and Eq. (3.9) are simular. Thus, we obtian

$$\mathsf{CV}^2[1 + 2\,\Xi] = C_v^2[1 + 2\sum_{i=1}^{\infty} \xi_i]. \tag{3.10}$$

The left hand side of Eq. (3.10) is indeed the Fano factor $\check{F}$ of the ensemble process as desired. Now, [Cox 1980] suggests as $k \to \infty$, $\mathsf{CV}^2 \to 1$. Interestingly, if all individual processes fullfill the renewal condition, it follows from Eq. (3.10) that $\check{F} = C_v^2 = [1 + 2\Xi]$, and therefore if $C_v^2 \neq 1$ the population activity is non-renewal with $\Xi < 0$ ($\Xi > 0$) for processes with $C_v^2 > 1$ ($C_v^2 < 1$). This important finding explains the numerical observation in [Lawrence 1973, Câteau 2006, Lindner 2006] regarding emergance of non-renewal processes as the result of the superposition operation.

3.5 Adaptation in a Neuronal Ensemble

In [Muller 2007] it has been shown by an adiabatic elimination of fast variables that the master equation description of a detailed neuron model including voltage dynamics, conductance-based synapses, and spike-induced adaptation reduces to a stochastic point process simular to Eq. (3.3). The corresponding hazard function can be approximated as

$$\hat{h}_x(x) = a_t \exp(-b_t x), \tag{3.11}$$

where a_t and b_t are determined by the time dependent statistics of inputs (see appendix A and the equilibrium rate consistency equation $r_{eq} \approx \hat{h}_x(r_{eq} q\tau)$ [Muller 2007] with the solution

$$r_{eq} = \mathcal{W}(abq\tau)/(bq\tau), \tag{3.12}$$

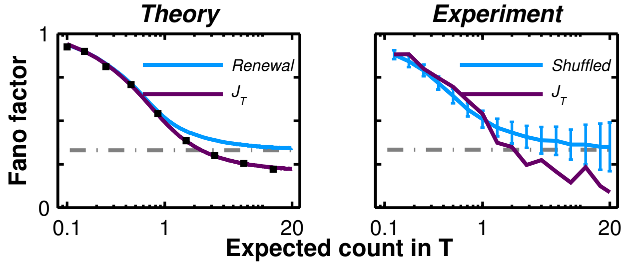

Figure 3.1: Adaptation reduces the Fano factor of the ensemble process. **Left** *Magenta*: J_T for arbitrary observation time T according to Eqs. (3.8) and (A.2) with $bq = 1.4$, $a = 5.0$ and $\tau = 400ms$. *Blue*: Fano factor for equivalent renewal ensemble process with interval distribution of Eq. (3.4). *Square Dots*: Numerically estimated Fano factor for superposition of the 5 realization runs of the full-detailed adaptive neuron model as in [Muller 2007]. *Dash-dotted line*: C_v^2. **Right** *Magenta*: Empirical $\hat{J}_T$ estimated from the pooled spike trains of 5 cortical neurons. *Blue*: Fano factor for the pool of shuffled spike trains. *Dash-dotted*: Average C_v^2 of the 5 individual spike trains.

where $\mathcal{W}$ is the Lambert function. In the case of vanishing adaptation ($bq \to 0$) the process apporaches the Poisson process with $r_{eq} \to a$.

We show in the appendix A that the adaptation dynamics in Eq. (3.1) produces negative serial correlations $\xi_k < 0$. The strength of serial correlation decays with increasing lag k and depends on the mean adaptation, $E[x] = r_{eq} q\tau$. Such a vanishing of negative serial interval correlations with increasing lag is well supported by a large body of experimental evidence [Farkhooi 2009b]. The departure from the renewal property induced by adaptation reduces the Fano factor Eq. (3.8) for the single process as well as for the population model of superimposed pocesses.

We validate our theoretical result of the reduced Fano factor in a set of experimental spike trains of $N = 5$ *in vivo* intracellular recorded neurons in the somatosensory cortex of the rat. The spontaneous activity of each of these neurons shows negative serial interval correlations [Nawrot 2007] where the empirical sum over correlation coefficients amounts to an average $\sum_{i=1}^{10} \xi_i = -0.28$. We construct the population activity by superimposing all 5 spike trains. Thereafter, we estimate the Fano factor as a function of the observation time and compare it to the case where, prior to superposition, renewal statistics is enforced for each individual neuron through interval shuffling. Our experimental observation in Fig. 3.1 (Right) confirms the theoretical prediction of a reduced Fano factor simular to individual neurons [Ratnam 2000] in the population level.

3.6 Benefits for Neural Coding

We provide three arguments that demonstrate how the mechanism of spike-frequency adaptation benefits neural processing and population coding. First, our result of a reduced Fano factor $\check{F} < C_v^2$ for the population activity of stationary adaptive processes ($bq > 0$) directly implies a reduction of the noise in the neuronal population rate code. Our analysis of a set of cortical data suggests a reduction of $> 50\%$ for long observation times. The reduction of J_T in Fig. 3.1 becomes significant even for small observation times of ≈ 2 average intervals, which is a relevant time scale for the transmission of a population rate signal. This result is reminiscent of an effect that has previously been acknowledged as noise shaping and weak stimuli detection expressed in the reduction of the low frequency power in a spectral analysis of spike trains with negative serial interval correlations [Chacron 2004, Fuwape 2008, Chacron 2001]. Our result confirms their findings at the population level.

Our second argument is concerned with the transmission of a population rate signal. We may define a functional neural ensemble by the common postsynaptic target neuron that receives the converging input of all ensemble members. To elucidate the postsynaptic effect of adaptation we simplify the ensemble autocorrelation function $A(u)$ following [Moreno-Bote 2008] with an exponential approximation

$$\hat{A}(u) = r_{eq}\delta(u) + [(F-1)/2\tau_c]\exp(-u/\tau_c), \tag{3.13}$$

where the second term is the approximation of $r_{eq}\mathcal{A}(u)$. For given observation time window u, and τ_c the reduction of F implies that $\hat{A}^r_u < \hat{A}_u$. Therefore, the postsynaptic neuron receives inputs from an adaptive ensemble that expresses an extended autocorrelation structure as compared to the inputs from a non-adaptive ensemble. Following the theory on the effect of input autocorrelation on signal transmission in spiking neurons as developed in [Moreno-Bote 2008, Moreno 2002], a longer τ_c reduces the input current fluctuations and this facilitates a faster and more reliable transmission of the modulated input rate signal by the postsynaptic target neuron.

Finally we argue that a postsynaptic neuron can better decode a small change in its input if the presynaptic neurons are adaptive. To this end, we compute the information gain of the postsynaptic activity, between two counting distributions of an adaptive presynaptic ensemble when $\hat{h}_x(x)$ is adiabatically transferred to $\hat{h}_x(x-\varepsilon)$ with a small change ε in the input ensemble. It is convenient to use $\tilde{\rho}_n(s)$ which associated with counting distribution $\tilde{P}(n,s)$. Thus, we apply the Kullback-Leibler divergence to the Eq. (3.6) before and after the adiabatic change in the input

$$D_{KL}(\tilde{\rho}^{\varepsilon}_n||\tilde{\rho}_n) = \textstyle\sum_i \tilde{\rho}^{\varepsilon}_i(s)\ln(\tilde{\rho}^{\varepsilon}_i(s)/\tilde{\rho}_i(s)). \tag{3.14}$$

Using Eq. (3.7) we obtain $D_{KL}(\tilde{\rho}^{\varepsilon}_n||\tilde{\rho}_n) = \mathcal{A}^{\varepsilon}_s[\ln(\mathcal{A}^{\varepsilon}_s/\mathcal{A}_s)]$. Due to Eqs. (3.1) and (3.12), the mean adaptation after the change is $E[x^{\varepsilon}] = \tau q r^{\varepsilon}_{eq}$. If $\varepsilon > 0$ it follows that $r^{\varepsilon}_{eq} \geq r_{eq}$. Therefore the mean adaptation level increases and the adapted process exhibits stronger negative serial correlations and $\mathcal{A}^{\varepsilon}_s > \mathcal{A}_s$. Thus, by Eq. (3.13), it is straight forward to deduce that $D_{KL} > D^r_{KL}$, for renewal and adaptive processes with identical interval distributions.

We now compute the information gain of the adaptive ensemble process relative to a matched Poisson rate model. For different initial rate values r_{eq} we assume a small but fixed increase ε in the input that we express in parameter changes a^{ε} and b^{ε} in Eq. (A.2) as outlined in appendix A. This leads to an increase $\kappa = r^{\varepsilon}_{eq} - r_{eq}$ in rate that is effectively constant over a wide range of initial values r_{eq} (Fig. 2, Left). In the rate model, assuming the same initial value of r_{eq}, the same input step leads

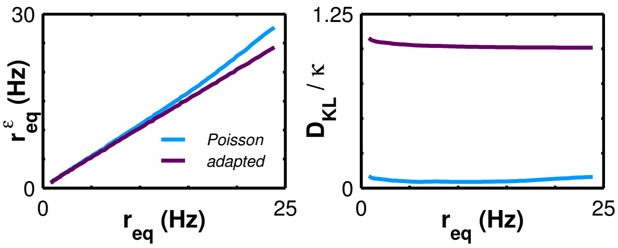

Figure 3.2: Information gain per spike due to adaptation. **Left**: Transfer of equilibrium rate for fixed ε change of the input in adaptive and Poisson model. **Right**: Kullback-Leibler Divergence per extra spike as the measure of information gain for n^{th} event density of adaptive and Poisson processes while $u = 200$ms and $\varepsilon = 0.01$nS with the same initial r_{eq} and $\kappa = r^{\varepsilon}_{eq} - r_{eq}$.

to a higher equilibrium rate increase $\kappa^{Poisson} > \kappa$, which depends on the inital rate (Fig. 2, Left) because the rate model lacks a mechanism of self-inhibition, which in the adaptive model counteracts the rate increase. Thereafter, we compute the Kullback-Leibler divergence for both models and normalize it by the change in the output rate κ. The result in Fig. 2 (Right) shows that D_{KL}/κ is larger for the adaptive model than for the rate model across the range of tested input rates. Thus, the information per extra spike is larger in the adaptive ensemble than in the renewal ensemble, and a postsynaptic neuron can discriminate small changes ε more efficiently, even though the absolute change in firing rate is lower.

3.7 Discussion

Our results point out a new aspect of spike frequency adaptation that benefits the reliable transmission and postsynaptic decoding of the neural population code. This aspect adds to the known properties of compression and temporal filtering of sensory input signals [Lundstrom 2008] in spike frequency adapting neurons. The specific result of Eq. (3.10) is also of practical consequence for the empirical analysis of the so-called multi-unit activity. By estimating Fano factor and serial correlations we readily obtain an estimate of the average C_v and serial correlation of the individual processes.

We developed a new formalism to treat event emitting systems that are influenced by a slow state variable, and we provide a number of useful general results on the higher order event statistics of superimposed renewal and non-renewal event processes, which are applicable to a wide range of event-based systems in nature, see appendic A . The derivation of the state dependent hazard and master equation [Muller 2007] assumes incoherent input fluctuation as in the mean-field theory, where common input is negligible. Treating a network with coherent fluctuations as encountered in finite size networks requires an alternative derivation of the hazard function as in appendix A.

3.8 Acknowledgments

We thank Carl van Vreeswijk and Stefano Cardanobile for valuable comments, and Clemens Boucsein for making the data available for re-analysis. This work was funded by the German Ministry of Education and Research (grants 01GQ0413 and 01GQ0941 to BCCN Berlin).

Chapter 4

Response Adaptation Can Explain Temporally Sparse Code in the Insect Mushroom Body[1]

The reconstruction of high dimensional signal representation patterns from limited numbers of measurements or sparse representation of a complex stimulus is central to neuroscience and system biology. Here, we established a relationship between an ubiquitously observed intrinsic response adaptation dynamics among the excitatory neurons and emergence of a temporal sparse code in the output of a network consist of them. Using a model of the insect olfactory system, we show that a simple mechanism of spike-frequency adaptation allows the explicit spare representation of stimulus in the population of Kenyon cells without extra inhibitory neuronal population. This explains a set of *in vivo* Ca-imaging experimental observations from Kenyon cells in the honeybee, where we find that blockage of inhibition does not alter the temporal sparseness reflected in the temporal dynamics of the signal. Furthermore, we show the successive adaptation in population level reduces the variability of responses and allows an efficient reconstruction; this founding may convey a fundamental characteristic of adaptive excitatory pathways of information processing in neuronal systems.

4.1 Introduction

Coding of highly complex sensory inputs with a sparse neuronal representation is a known coding scheme in many neuronal systems, for examples this coding is observed in the visual [Vinje 2000, Tolhurst 2009], auditory [Asari 2006, DeWeese 2003, Hromádka 2008], olfactory [Perez-Orive 2002, Poo 2009] and motor [Brecht 2004, Fiete 2004] pathways. Theoretically, sparse coding is desirable, because it allows for an efficient representation of the complex stimulus at any point in time with only a small number of vocabulary elements [Olshausen 2004]. This outline is specifically intriguing for formation of an associative memory architecture at later processing stages in the brain [Zetzsche 1990, Földiák 1995] and reminiscent of machine learning approaches that use dimensionality reduction [Palm 1980]. For populations of spiking neurons, sparse code implies that only very few active neurons code for a specific state, e.g. a particular stimulus configuration (population sparseness), and that each neuron represents information over time with only a small number of spikes per time unit (lifetime

[1] The material in this chapter is partly published in **Farkhooi, F., Muller, E. & Nawrot, M.** *Sequential sparsening by successive adapting neural populations*. **BMC Neuroscience 10, O10 (2009)**. The complete chapter will be submitted to a peer-reviewed international journal for publication under the same title and the following author list: **Farkhooi, F., Froese, A., Muller, E., Menzel, R. and Nawrot, M.P.**. Please refers to page iii in this dissertation for the detials of authors contributions.

sparseness). This, in turn, leads to low firing rates and low noise levels, as were described in review by Olshausen and Foldiak [Olshausen 2004].

Although the sparse coding strategy is known for many years, little is known about how spiking neurons produce filters that resemble the encoding in a sparse manner. Hereby, without loss of generality, we have addressed this issue in a network of insect olfactory system. In particular, we study, the sparse activity which is a fundamental aspect of neural code in Kenyan cells (KCs) in mushroom body (MB). It is known that KCs represent odors in the sense of population sparseness and additionally each response consist of a few spikes [Laurent 2002, Ito 2008, Szyszka 2005, Perez-Orive 2002]. The mechanism underlies the sparseness in KCs can be various, it is proposed to be possibly the mutual effect of network architecture [Jortner 2007] with interaction of inhibition and excitation component [Assisi 2007, Szyszka 2005] and sub-cellular biophysics of KCs [Laurent 2002, Demmer 2009]. Here, we propose an alternative mechanism that produces a temporal sparse code in KCs; due to a network effect of a generally observed intrinsic excitatory neurons phenomena, so called spike-frequency adaptation (SFA). The transduction of SFA is diverse in olfactory pathway for different insect and neurons [Kaissling 1987, Mercer 2002, Grunewald 2003, Wüstenberg 2004, Schafer 1994, Laurent 2002, Demmer 2009, Nagel 2011]; however, olfactory adaptation is qualitatively similar. We argue these sub-cellular mechanisms at the network level may underlies the temporal sparse code in the KCs. In principal, this effect resembles the compounding effects of successive adaptive populations. This suggests that progression of transient responses and high-pass filtering effects of SFA [Benda 2005] are amplified in successive adapting populations and lead to sparse code at KCs level. Additionally, a recent evidence by Kazama and Wilson [Kazama 2008] on short-term synaptic depression (STD) in the input to the principal excitatory cells in antenna lobe, so called projection neurons (PNs), which produces similar output profile. This acts in a qualitatively same filtering mechanism [Merkel 2010] and provides an alternative similar dynamics that possibly contributes to a degree of lifetime spareness in KCs.

We investigate further, the hypothesis of responses adaptation role to produce temporally spares code while *in vivo* inhibitory neuronal transmitters in honeybee brain are experimentally blocked. We found in a series of Ca-imaging experiments in the honeybee under abolishing GABA inhibition mechanisms, KCs time-course of activity remain unchanged which indicate the possible role of fast adaptation on temporal sparseness. This is likely to be a general mode for sparse coding also in other systems where the successive population of adaptive neurons are transmitting a transient like stimulus.

4.2 Materials and Methods

4.2.1 Experiment

Preparation and dye loading. Experimental procedures for *in vivo* calcium imaging were described in detail elsewhere [Haehnel 2009]. In brief, foraging honeybees (Apis mellifera) were caught at the entrance of the hive, immobilized, and fixed in a plexiglas chamber before the head capsule was opened for dye injection. We retrogradely stained either projection neurons (PN) or clawed Kenyon cells (KC) of the median calyx using the calcium sensor FURA-2 dextran (Molecular Probes, Eugene, USA) using a dye loaded glass electrode, which was inserted either into the lateral antenna-cerebralis tract (l-ACT) to stain PN axons [Sachse 2002] or into KC axons projecting to the ventral median part of the α-lobe [Szyszka 2005]. After dye injection head capsule was closed, bees feed and kept in a dark humid chamber for several hours. Before starting experiment, bees were further prepared as described earlier [Haehnel 2009], but here preparation has been modified by not covering the brain with silicon, instead bee brains were covered with ringer solution only.

Calcium imaging and Odor Stimulation. Experiments were performed following the method published elsewhere in [Haehnel 2009, Szyszka 2005] and the processing of imaging data was performed with custom written routines in IDL (RSI, Boulder, CO, USA). In summary, changes in the calcium concentration were measured as absolute changes of fluorescence; a ratio was calculated from the intensities measured at 340nm and 380nm illumination, the background fluorescence before odor onset was subtracted leading to ΔF with F = F340/F380. Odor stimulation were preformed Under the microscope, the naturally occurring plant odor octanol (Sigma Aldrich, Germany), diluted 1:100 in paraffine oil (FLUKA, Buchs, Switzerland), was delivered to both antennae of the subjects using a computer controlled, custom made olfactometer (adapted from Galizia et al., 1997). To this, odor loaded air was injected into a permanent airstream resulting in a further 1:10 dilution. Stimulus duration was 3 seconds if not mentioned otherwise. The air was permanently exhausted.

Pharmacology. A solution of 150 μl GABA antagonists dissolved in ringer for final concentration (10-5M picrotoxin (PTX, Sigma Aldrich, Germany) or 5x10^4M CGP54626 (CGP, Tocris Bioscience, USA)) were bath applied to the brain after pretreatment measurements. Next measurements started 10 min after drug application.

4.2.2 Network Simulation

Neuron model and simulator software. Our model neuron is chosen to be a general conductance-based integrated and fire with spike-frequency adaptation as it is proposed in [Muller 2007]. The model phenomenologically captures a wide array of spike-frequncy biophysical mechanisms such as M-type current, afterhyperpolarization (AHP-current) and even slow recovery from inactivation of the fast sodium current [Muller 2007]. The model neuron is also known to perform high-pass filtering of the input frequencies following the universal model of adaptation proposed by Benda and Herz [Benda 2003] with gain of

$$g(f_s) = f'_\infty \sqrt{\frac{1 + 2\pi f_s \tau_{eff} f'_0 / f'_\infty}{1 + (2\pi f_s \tau_{eff})^2}}, \tag{4.1}$$

where f'_0 and f'_∞ are the slopes of the $f - I$ curves, and f'_s is the frequency component of the stimulus [Benda 2005, Benda 2003]. Neuron parameters used for the production of plots can be reached at the simulation code at ModelDB[2]. The model used for the static synapses between the neurons in the SFA network simulations is conductance based alpha-shape with gamma distributed time constant from $\Gamma(2.5, 4)$ and $\Gamma(5, 4)$ for excitatory and inhibitory synapses, respectively. The dynamic synapses model with short-term depression (STD) also based on the phenomenological model introduced by Tsodyks et al. [Tsodyks 1998]. All simulations were performed using NEST simulator [Gewaltig 2007] version 2.0beta and Pynest interface [Eppler 2008]. The PyNest code for the model is freely available from ModelDB[3].

Network geometry and Connectivity. The model network consists of 1480 ORNs, 24 PNs, 4000 LN and 1000 KCs, thus keeping the ratio between the number neurons in olfactory pathway of honeybee as in [Menzel 2009]. The network connectivity is straight forward: each PN and LN receive excitatory connection from 20% randomly chosen ORNs [Sachse 2002, Chou 2010, Wehr 1996]. Additionally, every PN receives input from 50% randomly chosen inhibitory LNs [Sachse 2002, Chou 2010]. In our model the PNs do not excite one another and each PN output diverges to 50% randomly chosen KCs [Szyszka 2005, Assisi 2007, Jortner 2007]. We simulated the input to each ORN by a independent Poisson distributed events in the receptors level with background rate of 500Hz and an step intensity increase with 200Hz with the maximum uniformly distributed onset of 40ms represents the stimulus[Krofczik 2008]. Stimulus lasted one second and increased the firing rate of ORNs. We simulated odor repetition by rerunning the simulation.

Network Simulation Tunings. We tune all simulated network to have same spontaneous activity as reported previously: the spontaneous firing rate of ORNs set to 15-25Hz [Nagel 2011], LNs 4-10Hz [Chou 2010], PNs 4-12 [Krofczik 2008] and KCs 0.2-1.0Hz [Ito 2008]. This is achieved by tuning the synaptic weights in the network. We randomized the neurons parameters while tuning the background rate to make sure the result is valid in a wide parameter regime.

4.3 Results

4.3.1 Inhibition Blockage Experiment

In an extensive study, Szyzska et al. [Szyszka 2005] demonstrated that clawed KCs in the honeybee consistently show brief odor responses following stimulus onset reflecting the temporal sparseness of clawed KC population responses in the honeybee by means of Ca-imaging from populations of stained KCs [Szyszka 2005]. The models of feedforward and feedback inhibition (Figure 4.1) predict that blocking of inhibition should destroy/undermine the mechanisms by which KC odor responses are shortened. In a new set of experiments we tested this hypothesis by blocking inhibition/GABA

[2]At the moment of writing this dissertation the parameters' tables are not yet uploaded at http://senselab.med.yale.edu/ModelDB/

[3]At the moment of writing this dissertation the simulation code is not yet uploaded at http://senselab.med.yale.edu/ModelDB/

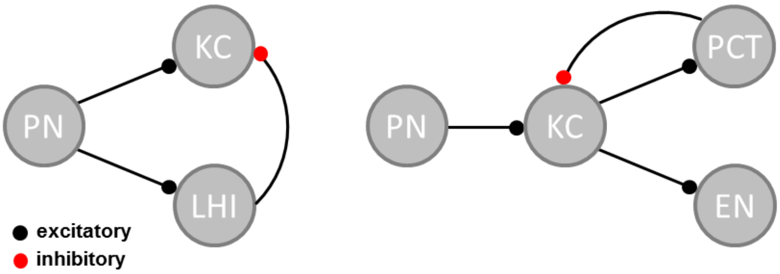

Figure 4.1: Hypothesis of feedforward and feedback inhibition for KC sparseness. **Left**: Model of feedforward inhibition. Following stimulus onset, the pool of PNs provides sustained excitatory input to the excitatory KC pool and to the inhibitory pool of lateral horn neurons (LHIs). The LHIs provide inhibitory input to the KC pool with a temporal delay Δt, which can truncate KC responses after only one or few spikes. This model was suggested based on anatomical evidence for the inhibitory connections between LHIs and KCs in the locust. **Right**: Model of feedback inhibition. PNs activate KCs, which in turn activate the inhibitory pool of PCT neurons and other excitatory MB extrinsic neurons (ENs). The PCTs provide inhibitory feedback to the KCs which arrives with a temporal delay $\Delta t'$ after the excitatory input.

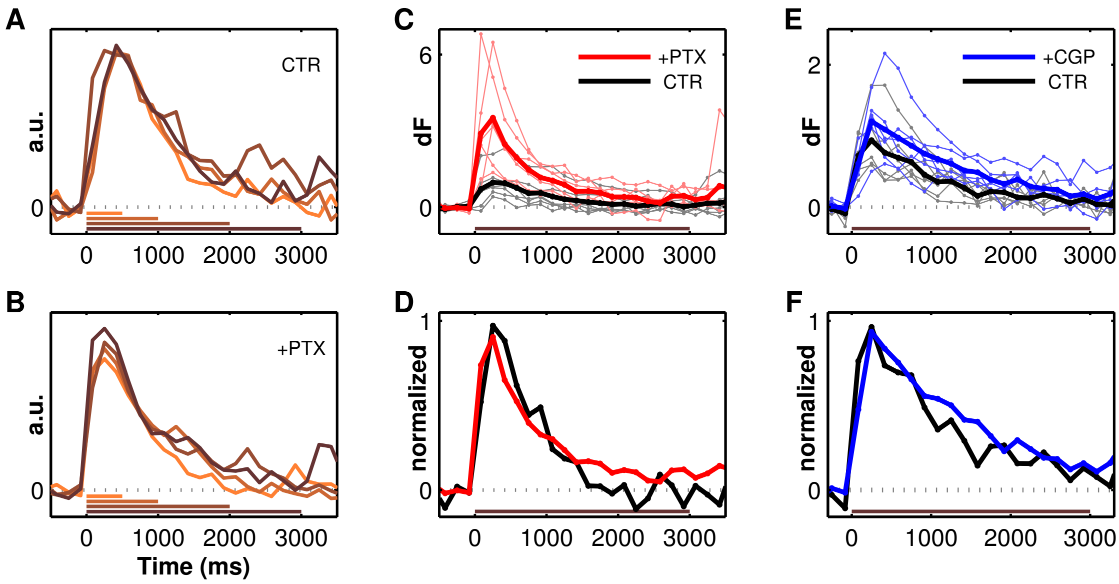

Figure 4.2: Blocking of GABAergic transmission changes amplitude but not duration of Ca response in the KC population. **A**: Temporal response profile of the Ca signal imaged from the MB lip region in one bee for stimulus durations of 0.5s, 1s, 2s and 3s, as indicated by color. **B**: Temporal response profiles as in (A) in one bee after application of PTX. **C**: Response profiles imaged from 6 control animals (gray) and their average (black) for a 3s stimulus as indicated by the stimulus bar. The responses measured in 6 animals in which GABA transmission was blocked with PTX (red) show a considerably higher population response amplitude. **D**: Average normalized responses are highly similar in animals treated with PTX (and control animals. **E**: Blocking GABA transmission with CGP in 6 animals (blue) again results in an increased response amplitude compared to 6 control animals (black). Average normalized response profiles are highly similar in CGP-treated and control animals. **F**: Dotted gray line indicates average baseline Ca activity before stimulus onset.

transmission and therefore repeated the Ca-imaging experiments from KC populations of the honeybee and tested the KC population responses when GABA inhibition was blocked (see Materials and Methods). Figure 4.2A shows the time-averaged and normalized across trials Ca-influx of population signal within the MB lip region during a 3s, 2s, 1s and 0.5s odor stimulus in a single bee. This indicates using different durations of the stimulus durations result in the same KC population response profile Figure 4.2A similar the time course of activity reported in [Szyszka 2005]; while the population response duration imaged from glomeruli in the AL shows a sustained activity throughout the odor stimulus / increased with increasing the stimulus duration [Sachse 2002], as it is reproduced in Figure 4.3B. In contrast to responses in AL, we found no differences between short (0.5s) and longer (3s) stimuli in KCs (Figure. 4.2). The calcium response recorded in the calyx was in all cases a brief phasic response at odor onset with a characteristic slope as previously reported by [Szyszka 2005]. This implies that the calcium response in KCs does not reflect the length of an odor application. Even shorter stimuli, ranging from 0.1 to 0.3 seconds, evoked the same response (data not shown). Further on, the bath application of PTX ($GABA_A$ blocker) as it is illustrated in Figure. 4.2 (B, C and D), this did not change the temporal dynamics of the responses. Here, also, we stimulated the animal with odor stimuli of different length, ranging from 0.5s to 3s, before and after systemic application of 10-5M PTX. The effectiveness of the drug was verified by the increased amplitude in response initial phase. However, we did not find any change in the temporal domain of the observed activity in the calyxes of 6 subjects. In addition to PTX, we tested the $GABA_B$ receptor blocker, CGP 54626 in a same protocol and found no elongated response after application of 5x10-4M CGP54626 (Figure 4.2E and F).

4.3.2 Population Response of Adaptive Network Simulations

In order to investigate effect of response adaptation on the sparse coding in network similar to result in population of KCs in insects; we performed different simulations on a simplified feedforward network to illustrate the possible role of adaptive responses due to the spike-frequency adaptation (SFA) and the short-term synaptic depression (STD) mechanisms for KCs spareness. Elsewhere, we suggested that mechanisms of self-inhibition provide an alternative hypothesis/model that could possibly explain temporal sparseness of KCs [Nawrot 2010b]. To test this hypothesis we conducted a set of neural network simulations of the insect olfactory pathway. Following the general network scheme outlined in [Menzel 2009]. we downscaled the total number of neurons in each layer keeping the relative numbers of neurons (see Materials and Methods). In a first set of simulations we assumed that LNs in the AL receive ORN input make homogeneous random connections to all/ fraction of PNs. We used the same spiking neuron model for all neuron types (ORNs, PNs, KCs). Importantly, this model is equipped with a mechanism for SFA [Muller 2007]. The SFA acts as a mechanism of self-inhibition: with each output spike it initializes a negative conductance of amplitude q_s = 2.1ns with a time constant of τ = 110ms for KCs, which is considerably longer than the synaptic time constants (range of $\tau = 100 - 500$ms is tested) (see

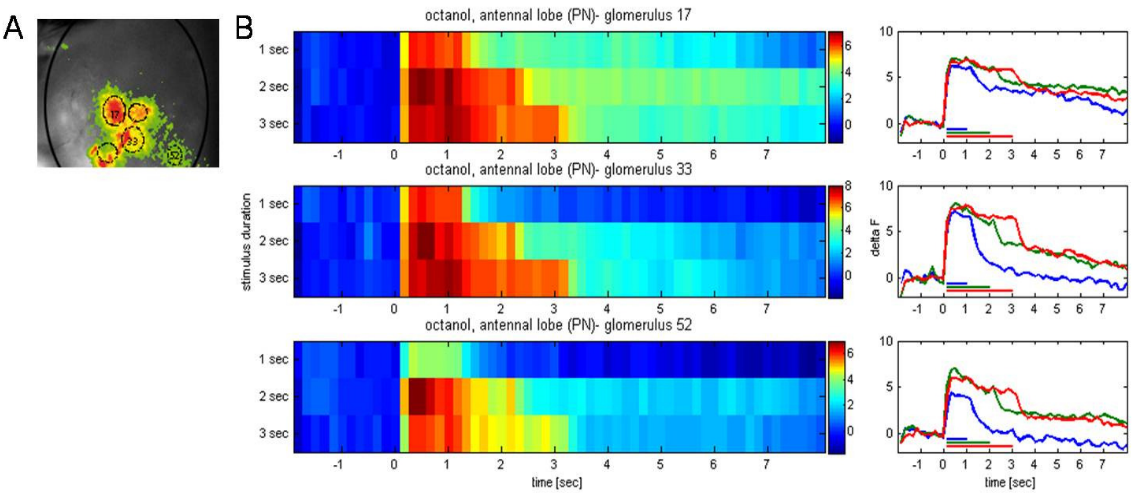

Figure 4.3: Different stimulus durations affect response length in PNs **A**: Raw fluorescence image of the antennal lobe, with false color coded responses during odor application, a subset of glomeruli numbered: 17, 33, 52. **B**: For each glomerulus (17, 33, 52) the response to an either 1, 2, or 3 second stimulus is shown as false color coded response traces, and as line plot (blue: 1s, green:2s, red:3s) [Froese 2009].

Materials and Methods). Thus, each action potentials has a long-lasting shunting effect and consequently can undermine excitatory input from the pre-synaptic PN population. The parameters (q_s, τ) defines the response properties of the neuron model [Muller 2007, Farkhooi 2011b] and were chosen differently for different neuron populations. The input to ORNs was modeled as a constant Poisson input during stimulus. For the PNs we chose $\tau = 110$ms which results in a dominant phasic-tonic response profile as demonstrated in Figure 4.4 (second row). As a result, upon receiving excitatory input from the PNs, KCs produce action potentials, which in turn lead to a strong self-inhibition and consequently to a rapid suppression of KC responses. The population response profile in Figure 4.4 resembles the experimental spike response profiles of KCs as in Figure 4.2. We measured also the temporal population sparseness using the Treves-Rolls population sparseness measure; it is argued [Willmore 2001] that this is a appropriate measure, since the response distributions are topically uni-modal and approximately symmetrical. Thus, we calculated

$$S_p = 1 - \frac{[\sum_j^N r_j/N]^2}{\sum_j^N r_j^2/N} \tag{4.2}$$

where N is number of neurons in the population and r_j and the number of spikes in the responses per time unit. In our first simulation the activity sparseness measure increased approximately two times, between PNs and KCs (Figure 4.4). In a second set of simulations we suppressed spiking in the inhibitory LN population. As to be expected this resulted in a larger population of active KCs and an increased population response Figure 4.4, third row. The population sparseness significantly decreased. Interestingly, the temporal response profile did not change but remained stable (compare Fig.4.4

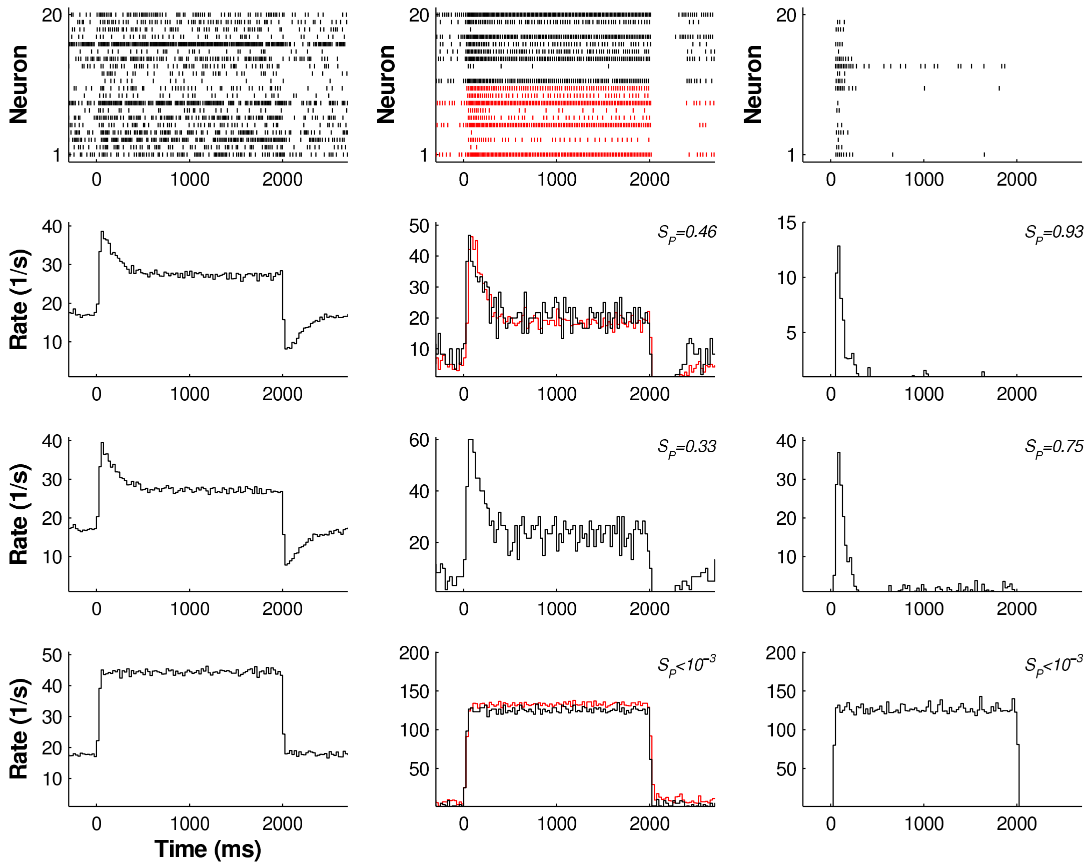

Figure 4.4: Average activity of the neuronal population in the simulated networks with the SFA. **First Row**: Randomly chosen spike trains of neurons in the simulated full network as it described in Material and Methods section. The ORNs, PNs, LNs(red) and KCs are left, middle, middle and right, respectively. **Second Row**: Propagation of activities a network equipped with SFA mechanism and local inhibition mirco-circuits with adaptation parameters $(2.1ns, 110ms)$ for ORNS and PNs and $(2.1ns, 110ms)$ for KCs. In the middle graph red line is the firing rate of LNs and all firing rate estimation has been done using 20ms bin. We set the adaptation of local inhibitory neurons very week. The temporal sparseness measure (S_p) for PNs is 0.46 and in KCs population is 0.96. **Third Row**: Propagation of activities a network similar to the first raw but without extra inhibitory population and the sparseness measure for KCs become $S_p = 0.75$. **Forth Row**: The same network of first raw while the adaptation parameters set to nil.

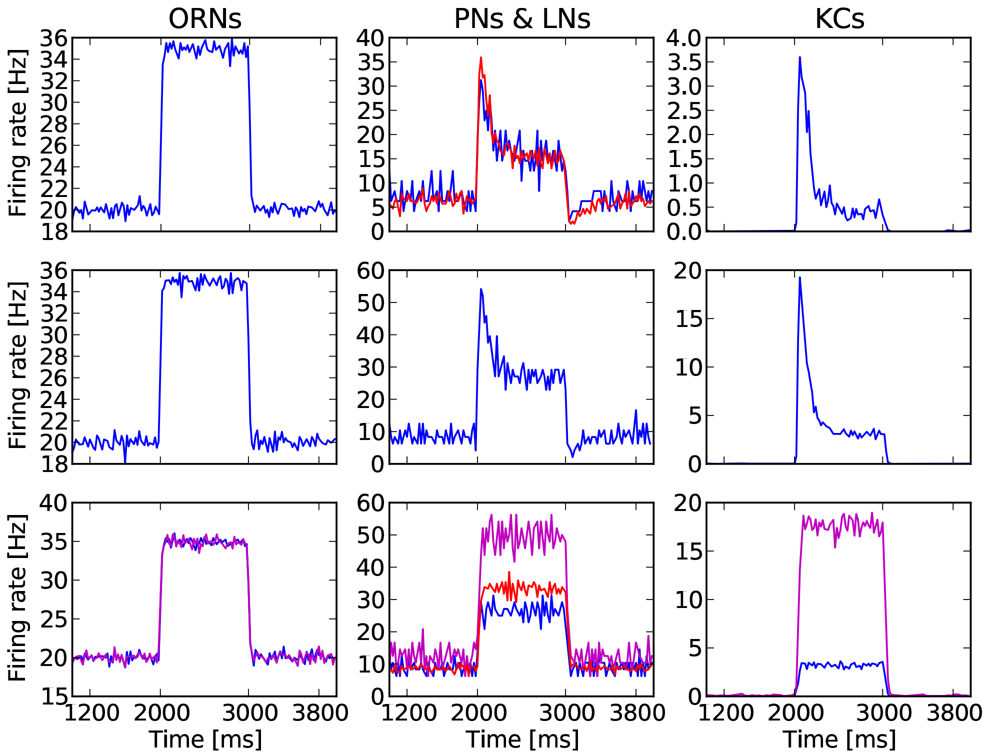

Figure 4.5: Average activity of the neuronal population in the simulated networks with STD. **First Row**: Propagation of activities a network equipped with STD mechanism and local inhibition micro-circuits in the ORNS→PNs connections with recovery time course of 900ms. In the middle graph red line is the firing rate of LNs and all firing rate estimation has been done using 20ms bin. The temporal sparseness measure (S_p) increase by 80% from PNs to KCs population. **Second Row**: Propagation of activities a network similar to the first raw but without extra inhibitory population. **Third Row**: The same network of first raw while the STD is disabled. In the middle graph the purple line is the firing rate of the PNs while the inhibitory neurons are ineffective.

second and third rows). Both results resemble our experimental findings from the Ca-imaging experiments.

As an alternative to the role of SFA, we simulate the network introduced in section above with non-adaptive neurons while dynamic synapses are implemented in ORNs→PNs as it is also experimentally suggested by [Kazama 2008]. The population responses of each layer presented in Figure 4.5 which support the temporally sparse KCs showed in Figure 4.2.

4.4 Discussion

We report here that the simple neuron-intrinsic mechanism of spike-frequency adaptation can account for the sparse spike response scheme known as lifetime sparseness [Willmore 2001] in downstream neurons. The SFA reflects high-pass filter properties with respect to the temporal profile of the neuron's input activity [Benda 2005, Benda 2003]. This suggests that a feedforeward network with the SFA neurons focuses on the temporal differences of the sensory input. In other words, it suggests that for higher brain centers it is most relevant to process dynamic changes in the sensory environment and to neglect the static receptor sensation. We designed our network model in coarse analogy to the insect olfactory system. Our model observation match with experimental observations. It clearly shows that the population response becomes increasingly phasic as it propagates through a network of the SFA neurons or a network with the STD connectivities which follows the experimental findings. However, in the control case where we switch off SFA or STD in all neurons or , the step-like input is conserved across all layers.

Generally, it was suggested that the successive adaptive stages employ a temporal differentiation of the sensory input in each processing layer similar to the findings in [Tripp 2009, Lundstrom 2008]. In the insect olfactory pathway this suggests that the representation evolves from stage to stage [Nawrot 2010b]. The input from ORNs are phasic-tonic and tonic [Nagel 2011, Kaissling 1987]. A phasic-tonic odor representation was observed in the PN population [Krofczik 2008, Namiki 2008, Nawrot 2010b] and it filters the input dynamics [Geffen 2009]. At the next stage, the KCs, the adaptive responses to the PN output results in a odor representation that strongly focuses on the dynamic changes in the input. This matches the repeated experimental observations in extracellular recordings from the locust and manduca (e.g. [Broome 2006, Ito 2008]) and imaging results in the honeybee [Szyszka 2005]. The natural environment provides time-varying olfactory scene. This has several factors: odor plumes (turbulences), air mass movement (wind), and autonomous animal behavior, the movement, in particular the flight of airborne insects, and the antenna movement that may compare to sniffing in mammals/rodents. In our model, a stimulus with time-varying amplitude will lead to a representation in the MB that strongly emphasizes the temporal changes in the input. Moreover, it is known that the SFA plays a significant role in helping up for patterning of response and synchronization along side with inhibitory cells [Sivan 2006, Assisi 2011] which has a high impact on odor coding in locust [Mazor 2005, Laurent 1999, Wehr 1996, MacLeod 1996]. Theoretically speaking, SFA has an extensive synchronizing-desynchronizing effects on population responses [Latham 2000, Fuhrmann 2002, van Vreeswijk 2000, van Vreeswijk 1994]. This mechanism is sharpen the possibility of synchronization population activity and that increases the elicitation of temporally sensitive responses in the later stage of processing.

In a resent study by Tripp et al. [Tripp 2009], it is shown that the filtering gain of a network with feed-forward response adaptation are principally works similar to a network with feed-forward delayed inhibition. However, the later circuits introduce greater errors than functionally equivalent feed-forward circuits. It is important to note the dynamics introduce in delay inhibitory networks operates in fundamentally different time-scales than response adaptive networks; since,these circuits are better suited for calculating the changes/derivatives of signals that evolve on time-scales outside the range of membrane and synaptic dynamics. Thus, co-existence of both provide a wide range of timescales needed for precise output sparse code in different time scale, fractional differentiation [Tripp 2009, Lundstrom 2008], spatial-temporal pattering of the sensory input [Assisi 2011], flexible gain control [Mar 1999] and dynamic information transmission in networks [Ávila-Åkerberg 2009, Ávila-Åkerberg 2010].

Our results here bears consequences for general coding. The regularizing effect of self-inhibition reduces the trial-to-trial variability not only of single neurons but also of the neuronal population that provides the input to downstream neurons. This improves detectability of weak signals and discriminability of different inputs [Farkhooi 2011b].

4.5 Acknowledgements

We are grateful to Michael Schmuker and Evern Pamir for valuable discussions on data and models and Neloy Kumar for his comments on the manuscripts. We acknowledge generous funding from the Deutsche Forschungsgemeinschaft (SFB 515), and from the German Federal Ministry of Education and Research (BMBF) to the Bernstein Center for Computational Neuroscience Berlin (01GQ0413).

Chapter 5

Discussion

In all living organisms, the systems have evolved to perform tasks in a specific contexts; many of these tasks are universal, while the solutions may be organism-specific [Nemenman 2010]. One of the most common universal functions performed by organisms at all levels of their complexity is signal and information processing to shape a relevant response. This requires the ability to distinguish signals in a noisy environment, whether the noise is extrinsic or generated by internal stochastic molecular mechanisms. In this regard, the nervous system plays a considerable role in signal processing, since it is widely known that many relevant biological features of tasks are processed in the organization of spiking neurons [Nemenman 2008, Laughlin 1981]. However, neural spiking activities exhibit a wide range of variability on various time scales [Nawrot 2010a]. While the function of this variability is still being debated [Stein 2005], it is generally agreed, that it is a fundamental aspect of spiking data *in vivo* conditions. Therefore, understanding the nature and origin of neuronal variability at both single cell and *in vivo* network levels might be of crucial importance for formulating theories about information processing in the nervous system under the condition of intrinsic and extrinsic noise [Destexhe 2003, London 2010]. In this dissertation, it is assumed that variability in the nervous system is an essential component of theories in sensory coding, learning and memory across the spiking neurons in the nervous system.

To measure and understand the variability in spiking data motivated research, it is frequently assumed as a simplification conceptual link, that neural activity *in vivo* conditions can be described by the distribution of inter-spike intervals [Moore 1966, Perkel 1967a, Perkel 1967b, Shadlen 1998, Bastian 2001]. This allows a quantification of variability in firing patterns of both peripheral and central neurons estimating coefficient of variation C_v and Fano factor variability F_T, where both provide a measure of variability and irregularity of the neurons, respectively [Nawrot 2008, Churchland 2010]. However, as it is shown in chapter 2, the statistical description of variability by assuming a renewal process is essentially not complete and generally neurons violate renewal assumptions. There is accumulating evidence that non-renewal patterning (e.g. oscillations, bursting and adaptation) in spike trains contain important information for neuronal information processing [Ávila-Åkerberg 2011]. In particular, it is shown in this dissertation that non-renewal statistics emerge from spike-frequency adaptation mechanisms in a variety of excitatory neurons. These mechanisms do not only alter spike timing, but also have non-mutual and exclusive functional consequences on variability, signal detection, coding capacity and gain control of both at single cells and networks' level.

The seminal work by Brik [Birk 1972] on a spinal motor neuron showed that the decoded representation of spike trains with negative inter-spike interval correlations displays less variability than a spike train with the same firing rate but with independent inter-spike intervals. In numerical simulations by [Ratnam 2000, Chacron 2001], it is demonstrated that a spike train with negative correlations among inter-event intervals displays less count variance than that of spike trains with independent inter-spike intervals. In cortical cells there is also accumulating evidence that negative serial correlation is the source of reduced variability [Nawrot 2007]. The numerical investigation of the statistical model in chapter 2 also confirms the effect of altering spike position due to the serial correlations on the counting process variance for single spike train. This result according to chapter 3 can be extended to the reduction of variability in the ensemble activity of a population of independent neurons. It directly implies a reduction of the noise in the neuronal population rate code. The analysis of a set of cortical data in chapter 3 suggests a reduction of 50% over a long observation time. This reduction is also significant even for a relatively short observation window of two average intervals, where it reduces the post-synaptic fluctuation according to analysis reported in chapter 3. This result is a reminiscent of an effect that has been acknowledged before as noise shaping for single spike trains [Chacron 2001, Longtin 2003] in a population of independent neurons. In short, noise shaping is expressed in the reduction of the low frequency power in a spectral analysis of spike trains with serial correlations. An interesting founding by [Prescott 2008] reveals that conventional noise shaping improves efficient spike-rate coding at the expense of a spike-timing code by regularizing the spike train elicited by slow or constant inputs. They used the activation of low threshold adaptation mechanisms or sub-threshold adaptation to stop the neuron from spiking repetitively to slow inputs and hence the model could generate isolated and well timed spikes in response to fast inputs as well [Prescott 2008]. Therefore, it can be argued that different biophysical mechanisms of spike-frequency adaptation can shape the noise power in a desirable manner to obtain reliable signal transmission. This can also be achieved alternatively with a more complicated network of neurons coupled with inhibitory feedbacks [Mar 1999].

Following the reduction of noise in the rate code, negative serial correlation facilitates detection of weak signals and increases the statistical power of discriminability for small changes in the input to neurons [Chacron 2001, Brandman 2002, Goense 2003]. The improvement of weak signal detection implies that spike-frequency adaptation increases the mutual information between output and input for a certain range of stimulation frequencies due to reduction of output entropy as a result of negative serial interval correlations. This idea is confirmed by Chacron et al. [Chacron 2001] who found that although negative inter-spike interval correlations reduce signal entropy, it also reduces the noise entropy with a greater magnitude, thereby increasing the mutual information. This phenomenon was first shown in the context of information processing in fly photo-receptors [Laughlin 1981]. A recent study by [Nesse 2010] has shown that optimization of mutual information depends on baseline activities and under the conditions that adaptation is not pronounced, the mutual information may significantly decrease. However, the analysis in chapters 2 and 3 demonstrate that the mechanisms of spike-frequency adaptation that give rise to non-renewal spike train statistics alter spike timing and also all moments of counting process and therefore facilitates decoding of small changes in the input. The effect in all moments of counting process can be in seen the distance between two count distributions with small differences in their input level, measured with Kullback-Leibler divergence. The distance indicates that an adaptive process contains more information in comparison to the equivalent renewal process with identical inter-event interval distribution. Therefore, the mutual information loss as it is argued by [Nesse 2010] does not hinder the better separation of two count distributions with small differences in their input level and thus it leads to a better signal detection or/and transmission. In an alternative scenario in chapter 3, where the effect of adaptation on rate is also considered, an equivalent renewal process could increase its rate without the boundary of self-negative feedback of adaptation in the response to an adiabatic change in the input level. Therefore, one can argue that the separation of two count processes is more efficient for the renewal spiking model, based on the argument that the distance between two counting processes (information gain) is much higher due to higher difference in their mean firing rate. However, this scenario is not realistic as neurons constrain with the number of action potential in a short time interval, thus normalizing the information gain per extra spike results in greater information transmission per spike for adaptive process e.g. chapter 3. This founding would then act synergistically and leads to a better separation of two count distributions for neurons with small differences in their inputs and a more efficient signal detection and transmission. Consequently, this affects an increase in the coding capacity (chapter 3); due to a better separation of two counting processes for adaptive ensembles. The model for population analysis of adaptation here is principally a cortical network model [Muller 2007]. Briefly, the master equation in chapter 3 and its time transformed form therein, are derived by an adiabatic elimination of fast variables from a more generalized master equation for the neuronal cortical field [Muller 2007]. The more general master equation here is given in Eq. (B.1) [Muller 2007] which assumes incoherent fluctuation in the network: The assumption is that a neuron in the network samples its input from an infinite reservoir of other neurons sparsely, therefore they share a negligible portion of common input; moreover it is also assumed that the network heterogeneity, and other sources of quenched randomness affecting the interaction in the network and effectively decorrelating firing probabilities. Based on these assumptions, the fluctuation in other variables are fast and will be eliminated. Interestingly, the hazard function in chapter 3 based on the approach by [Muller 2007] is the response function of the system in the mean-field theoretical formalism as it has been derived by [Siegert 1951, Buonocore 2010, Brunel 2000] using the Fokker-Plank approximation. Although this approach provides valuable methods for analytical treatment of adaptation in population level, it fails when there is sufficient cross-correlations within the network. A well known case, where the interaction in the network is not negligible is the network with a finite size. In this regard, one needs to adopt the master equation with system size expansion as it is develop by [Bressloff 2009]. Despite of its complexity of analysis, this direction of research may reveal how noise in the single cell level translates into the noise at a population level for more realistic biophysical models. The other condition where network spike-spike cross-correlation is limiting the results here is the all-to-all networks. To account for such situations, two recent studies have explored the interesting effect of adaptation in highly correlated all-to-all networks [Ávila-Åkerberg 2009, Ávila-Åkerberg 2010]. These studies showed that renewal and adaptive neurons transmit information differentially. In summary, adaptive networks with excitatory/inhibitory coupling transmit more/less information than networks with renewal neurons of the same size without coupling. In contrast, renewal networks with excitatory/inhibitory coupling transmit less/ more information than renewal networks of the same size with no coupling. As such, excitatory and inhibitory couplings each have opposite effects on networks of renewal and non-renewal model neurons. As anatomical studies have found that the majority of synaptic connections in the brain are excitatory, it is possible that such connections increase information transmission by neurons that display non-renewal spike train statistics [Ávila-Åkerberg 2011].

The emergence of gain control due to slow dynamics of adaptation in a single cell is another very important property of spike-frequency adaptation [Benda 2003]. Mechanistically, adaptation acts subtractively on the input into the neuron and adds a high-pass filter to the neuron's transfer function [Nelson 1997, French 2001, Benda 2005]. A high-pass filter attenuates slow stimulus components including the mean, whereas fast stimulus components are transmitted with high gain [Benda 2007]. Ideally, under the condition that the slow stimulus components were suppressed completely, the response to fast components will be independent of the mean intensity of the stimulus. Therefore, the response of such a neuron will be intensity invariant [Benda 2007]. It is also argued that the high-pass filtering properties of adaptation rescale the dynamic range of the responses to that of the stimulus and maximizes information transmission [Borst 2005]. It has been also shown that the ideal case of an adaptation high-pass filter is achievable in a theoretical sense [Tripp 2009]. However, experimental evidence shows adaptive neurons only do a fractional high-pass filter [Lundstrom 2008]. Therefore, the ideal case of intensity invariant responses cannot be achieved at a single cell processing level, it may need a network architecture to produce such useful coding scheme. In this regard, in chapter 4 a complementary aspect of adaptation filtering effect in the network is studied. It is evidently shown that a feed-forward network of adaptive neurons can produce an stable and an efficient sparse representation of stimulation across the full possible range of parameters conditions. This results contributes to recent theoretical and experimental evidence indicating that many sensory neural systems appear to employ similar sparse representations with their population codes [Vinje 2002, Lewicki 2002, Olshausen 1996, Olshausen 2004, Delgutte 1998, Assisi 2007], encoding a stimulus in the activity of a few neurons and/or a few spikes. Specifically, in chapter 4, it is proposed that neuronal spike-frequency adaptation mechanisms might play a considerable role in temporal sparseness of a sub-population of insect mushroom-body principal neurons, so called Kenyon cells. This hypothesis is supported with experimental observations of Kenyon cells activity [Ito 2008, Szyszka 2005, Perez-Orive 2002] and physiological founding of adaptation mechanisms in the insect olfactory network [Mercer 2002, Grunewald 2003, Wüstenberg 2004, Schafer 1994, Laurent 2002, Demmer 2009]. Further on, the role of short-term synaptic plasticity in the network sparseness is also alternatively investigated, where comparably similar qualitative results to the dynamics of spike-frequency adaptive neurons are shown. Using computer simulations, it is shown that changes in synaptic resources and/or level of adaptation in feed-forward networks of receptor neurons, projection neurons and Kenyon cells adjust their window of integration to produce sharp sparse code in the output. In general, this simple neuronal intrinsic adaptive mechanism may be useful for maintaining sparseness of sensory representations across wide ranges of stimulus conditions. This effect might hint a new insight towards the prospect that it is in fact these transient responses which are the signals, and thus they may interpret synchrony and/or signal amplification [Muller 2007, van Vreeswijk 2000], which in principal contribute to the result on noise reduction as discussed earlier in this chapter. This approach provides an alternative model to the previous feed-forward inhibition mechanism that has been suggested to produce a desirable sparse code [Assisi 2007]. The lacking study here can be the incorporation of beyond mean-adaptation theories to study the likely effect of adaptation temporal variance [Buiatti 2003, Nemenman 2010] on the sparseness of Kenyon cells in experimental conditions.

Closing remarks. The topics in this dissertation point out the importance of non-renewal statistics for neuronal dynamics in excitatory cells which has been largely ignored in neural ensemble studies. It incorporates a rigorous treatment of non-renewal population density framework to derive useful results on effects that emerge from beyond renewal spiking statistics of neurons. Given the variety of intriguing and prominent consequences such as inter-spike interval correlations and regularization of activity by reduction of variability and thus signal transmission, amplification and filtering effects of transient responses in successive populations, alongside with strong altering of temporal frequency tuning [Ellis 2007, Mehaffey 2008, Lindner 2009, Peron 2009, Cortes 2011]; it is completely unlikely that spike-frequency adaptation can be neglected in many neuronal phenomenon. Here, it can be argued that spike-frequency adaptation maybe have drastic effects when considering, for example, the dynamic nature of the neural code [Shadlen 1998], the propagation of synchrony [Abeles 1991, Diesmann 1999, Kumar 2010], or the function of spike-timing based learning rules [Gerstner 1996, Song 2000, Clopath 2008]. To tackle these questions we are lacking a good approximation of *in vivo* like networks with coherent fluctuation and non-Markovian time delays to take into account some aspects of the ensemble context of many neuronal interactions. This requires a generalization of perturbation analysis similar to van Vreeswijk's work [van Vreeswijk 2000] in a network level and their variability measures of time dependent input to answer fundamental questions: how does noise at a cellular level translate to population level and propagates to the post-synaptic population with synaptic dynamics? And how memories are sustained in biological systems with a significant variability?

Appendix A

Hazard Function and Process Serial Correlations

A.1 State-Dependent Hazard Function

We define a limiting probability density to an event, given the state variable x, as

$$h_x(x,t) := \lim_{\varepsilon \to 0} \frac{\Pr(N[t, t+\varepsilon] > 0 | x(t))}{\varepsilon}, \tag{A.1}$$

where $N[t, t+\varepsilon]$ is a right continuous integer-valued function that jumps 1 at each event time and is constant otherwise. Thus, $N[t, t+\varepsilon]$ counts the number of events in the interval $(t, t+\varepsilon]$, and x is a general state variable of the system. Here, we assume a shot noise dynamics as described by Eq. (1) in the main text governs the state variable x.

The hazard function for neuronal ensembles can be derived from a field master equation of the system as it is stated in Eq. (B.1) [Muller 2007]. Generally, a full master equation assumes an infinite reservoir of entities and sparse interaction among them (the underling assumptions of mean-field theory). Therefore, it results that the fluctuation in the inputs are incoherent and sufficiently uncorrelated. This allows to apply the method of elimination of fast variables [Gardiner 1984] given the slow state variable x [Muller 2007]. Indeed, it can be shown that the hazard function is the response function of a neuron in the presence of noise, which can be derived by the Fokker-Planck approximation of the mean field master equation [Siegert 1951, Brunel 2000] as described in [LaCamera 2004] for mean-adaptation theory.

In [Muller 2007] it is shown that the Kramer rate function [Gardiner 2004]

$$\hat{h}_x(x,t) = a_t \exp(-b_t x) \tag{A.2}$$

provides an excellent agreement with the mean field calculation of the response function, where a_t and b_t are fit parameters to the full model of a neuron including voltage dynamics and conductance-based synapses. In a dynamic input setting a_t and b_t are respectively determined by interpolating the mean excitatory and inhibitory synaptic conductance to the neuron (see section 3 and 4 in [Muller 2007]). In a static case, a_t and b_t denote as a and b, respectively. Moreover, the effect of input statistics and varying noise strength on Eq. (A.2) and the resulting inter-event distribution is studied in [Nesse 2008]. In summary, a corresponds to firing rate of a neuron given the statistics of input parameters, where $x = 0$, and b is the adaptation coefficient otherwise and can be derived using adaptation self-consistency in Eq. (13) in the main text. This relationship allows to construct the rate model as in the main text (last argument in Section *Benefits for Neural coding*), where a and b are derived using the fit provided in NeuroTools [1]. It is clear from Eq. (A.2) that without adaptation a is the firing rate of the Poisson rate model. In order to allow comparison, we normalized both processes to have the same initial firing rate (Fig. 2) by assuming that there exists some constant regulation $0 < \mathcal{N} < 1$ that maintains rate equality in the steady-state such that

$$r_{eq} = a\mathcal{N} = \mathcal{W}(abq\tau)/(bq\tau). \tag{A.3}$$

Thereafter, we assumed a change ε in the mean conductance on the order of 0.01 nS and recompute a^ε and b^ε, thus the rate model new equilibrium rate is $\bar{r}^\varepsilon_{eq} = a^\varepsilon\mathcal{N}$. The new equilibrium rate of the adaptive process is obtained by $r^\varepsilon_{eq} = \mathcal{W}(a^\varepsilon b^\varepsilon q\tau)/(b^\varepsilon q\tau)$. This construction leads to Fig. 2 (Left) in the main text.

A violation of the mean-field theory assumptions, such as a finite size of reservoir, in the network bring about "coherent" fluctuations in addition to "incoherent" fluctuations, both can be used to derive the response function of the system [Mattia 2002, Bressloff 2009], which implicates an alternative form for the hazard function which includes a stochastic element [Mattia 2002]. However, under the condition that the correlation time course of the interactions is short compared to adaptation time scale, namely on the order of the synaptic time constant, interactions can be treated as fast variables and, in the presence of slow adaptation, will vanish by the method of elimination of fast variables.

The hazard function has been derived for many physical systems. We mention the examples of models for earthquake events [Corral 2005], financial risk modeling in econophysics [Katz 2010]. It is also plausible to apply the adiabatic elimination technique for quantum dissipative system to obtain a matching hazard model as suggested in [Casagrande 1985].

A.2 Serial Correlation: Process memory

The history dependency of the slow dynamic shot-noise in Eq. (1) of the main text, results in a state-dependent reset mechanism ψ which makes the process non-renewal. Since the state variable $x(t)$ when an event occurs, makes a jump $x(t + dt) = x(t) + q$ defining the reset mapping $\psi(\eta(x))$, such that the reset condition become $\eta(x) \mapsto \eta(x + q)$, it follows that

$$\psi(t_x) = \eta(\eta^{-1}(t_x) + q) = -\tau \ln(\exp(-t_x/\tau) + 1) \tag{A.4}$$

with its inverse given by

$$\psi^{-1}(t_x) = -\tau \ln(\exp(-t_x/\tau) - 1). \tag{A.5}$$

It is clear that at the time of event, state variable remapping condition deviates from $t_x \mapsto 0$. However, if we assume $q = 0$, it results second and third terms in right hand

[1] http://neuralensemble.org/trac/NeuroTools

side of Eq. (2) canceling each other, which makes the master equation follows a renewal theory and non-locality due to q vanishes.

Therefore, the state-dependent reset ψ indicates the memory of the process in the terms of serial correlation between consecutive inter-event intervals. Here, we shall now relate the interval correlation coefficient to the probability of observing n events in the time window T, $P(n,T)$, using the relationships derived in [McFadden 1962]. Hence, the correlation of two back to back intervals is

$$\int_0^\infty P(1,T)dT = \lim_{s\to 0} \tilde{P}(1,s) = E[\Delta_0\Delta_1]/\mu_1 \tag{A.6}$$

and similarly for k lagged intervals, we have $\tilde{P}(k,0) = E[\Delta_0\Delta_k]/\mu_1$ [McFadden 1962].

Here, we show that serial correlations between inter-events are negative for phenomenological model of adaptation, following the distribution given in Eq. (4) and its corresponding counting process $P(n,T)$, for a given hazard function as Eq. (A.2) and defined ψ in the main text for a static firing rate: As ψ only operates on the current state and the reset at the k^{th} interval before has a vanishing effect on the current state of t_x, we have $\lim_{k\to\infty} \rho(\Delta_0,\Delta_k) = \rho(\Delta_0)\rho(\Delta_k)$ [Muller 2007]. Therefore, applying Lemma (6.5) in [McFadden 1962] $\lim_{k\to\infty} \tilde{P}(k,0) = \mu_1$. Additionally, since $\psi : \mathbb{R} \mapsto \mathbb{R}^-$, it follows that all trajectories are reinserted at negative pseudo-ages, and we have $\partial_{t_x}\psi < 0$, therefore "younger" event trajectories are reinserted at more negative values and hazard function that explicitly defined in Eq. (A.2) is an increasing $\partial_{t_x}\hat{h}_x(\eta(x)) > 0$. Hence, for a given μ_1 it follows that neuronal adaption model here has the property $\mu_1^2 \geq E[\Delta_0\Delta_k]$. Thus, the correlation coefficient ξ_k between two intervals separated by lag k is negative and dies out for large values of k.

Generally, following the same argument, if ψ and h are monotonous and

$$\partial_{t_x}\psi(t_x)\partial_{t_x}h(t_x) < 0 \tag{A.7}$$

then the intervals exhibit a negative serial correlation. The condition on the Eq. (A.7) also indicates that if $\partial_{t_x}\psi(t_x)\partial_{t_x}h(t_x) = 0$ the process is renewal and under the condition of

$$\partial_{t_x}\psi(t_x)\partial_{t_x}h(t_x) > 0 \tag{A.8}$$

process produces positive serial correlation.

A.3 Serial Correlations Beyond the Neuronal Systems

In this letter, we show that the negativity of serial correlation in neural adaptation enhances the signal transmission. Moreover, it has been argued that a sub-Poissonian statistics ($C_v^2 < 1$) is superior for light communication systems because it exhibits reduced variability the count statistics as compared to the Poisson statistics [Saleh 1987, Jann 1996]. The phenomenon of negative serial correlations (Eq. (A.7)) is also observed in multi-level quantum systems [Soler 2008] where $\mathcal{M}$ measures the serial correlation between consecutive inter-photon times. According to our results, a

Table A.1: Neuron model parameters as it is used for simulations of the full model neuron with voltage dynamics, adaptation and conductance-based synapses [Muller 2007], as illustrated in Fig. 3.1. The simulation is performed in PyNEST [Eppler 2008].

Parameter	Description	Value
v_{th}	Threshold voltage	-57mV
v_{reset}	Rest voltage	-70mV
c_m	Membrane capacitance	289.5pF
g_l	Membrane leak conductance	28.95pS
E_l	Membrane reversal potential	-70mV
q_{rr}	RELREF quantal conductance increase	3214nS
τ_{rr}	RELREF conductance decay time	1.97ms
E_{rr}	RELREF reversal potential	-70mV
q_s	SFA quantal conductance increase	14.48nS
τ_s	SFA conductance decay time	110ms
E_s	SFA reversal potential	-70mV
$E_{e,i}$	Reversal potential of excitatory and inhibitory synapses, respectively	0 mV, -75mV
$q_{e,i}$	Excitatory and inhibitory synaptic quantal conductance increase	2nS
$\tau_{e,i}$	Excitatory and inhibitory synaptic decay time	1.5ms , 10ms
$\lambda_{e,i}$	Excitatory and inhibitory input rate	6Hz, 11.4Hz

superposition of non-renewal photon emitters could enhance reliable information transmission and signal discrimination in photo detecting devices.

The condition in Eq. (A.8) might be of interest for event emitting systems that exhibit a self-exciting feedback and thus depart from renewal assumption by positive serial correlations between adjacent inter-event intervals. For example, it has been shown in [Livina 2005] that after major earthquakes the rate of the aftershocks decreases in time by the Omori law. This decreasing rate generates a memory of inter-events where small (large) recurrence intervals follow small (large) ones, implying positive correlations among inter-event times.

Bibliography

[Abeles 1991] Moshe Abeles. Corticonics: neural circuits of the cerebral cortex. Cambridge University Press, February 1991. 47

[Arieli 1996] A. Arieli, A. Sterkin, A. Grinvald and A. Aertsen. *Dynamics of ongoing activity: Explanation of the large variability in evoked cortical responses*. Science, vol. 273, no. 5283, pages 1868–1871, 1996. 19

[Asari 2006] Hiroki Asari, Barak A. Pearlmutter and Anthony M. Zador. *Sparse Representations for the Cocktail Party Problem*. The Journal of Neuroscience, vol. 26, no. 28, pages 7477 –7490, July 2006. 32

[Assisi 2007] Collins Assisi, Mark Stopfer, Gilles Laurent and Maxim Bazhenov. *Adaptive regulation of sparseness by feedforward inhibition*. Nat Neurosci, vol. 10, no. 9, pages 1176–84, September 2007. 4, 33, 35, 46, 47

[Assisi 2011] Collins Assisi, Mark Stopfer and Maxim Bazhenov. *Using the Structure of Inhibitory Networks to Unravel Mechanisms of Spatiotemporal Patterning*. Neuron, vol. 69, no. 2, pages 373–386, January 2011. 41, 42

[Ávila-Åkerberg 2009] Oscar Ávila-Åkerberg and Maurice J. Chacron. *Noise shaping in neural populations*. Physical Review E, vol. 79, no. 1, page 011914, January 2009. 42, 46

[Ávila-Åkerberg 2010] O. Ávila-Åkerberg and M. J. Chacron. *Noise Shaping in Neural Populations with Global Delayed Feedback*. Mathematical Modelling of Natural Phenomena, vol. 5, no. 2, page 25, 2010. 42, 46

[Ávila-Åkerberg 2011] Oscar Ávila-Åkerberg and Maurice J. Chacron. *Nonrenewal spike train statistics: causes and functional consequences on neural coding*. Experimental Brain Research, 2011. 2, 43, 46

[Barbieri 2001] Riccardo Barbieri, Michael C Quirk, Loren M Frank, Matthew A Wilson and Emery N Brown. *Construction and analysis of non-Poisson stimulus-response models of neural spiking activity*. J Neurosci Methods, vol. 105, pages 25–37, 2001. 6

[Bastian 2001] Joseph Bastian and Jerry Nguyenkim. *Dendritic Modulation of Burst-Like Firing in Sensory Neurons*. Journal of Neurophysiology, vol. 85, no. 1, pages 10 –22, January 2001. 2, 43

[Bear 2006] Mark F. Bear, Barry W. Connors and Michael A. Paradiso. Neuroscience: Exploring the brain. Lippincott Williams & Wilkins, third édition, February 2006. 1

[Benda 2003] Jan Benda and Andreas V. M. Herz. *A Universal Model for Spike-Frequency Adaptation.* Neural Computation, vol. 15, no. 11, pages 2523–2564, November 2003. 1, 3, 34, 35, 41, 46

[Benda 2005] Jan Benda, Andre Longtin and Len Maler. *Spike-Frequency Adaptation Separates Transient Communication Signals from Background Oscillations.* J. Neurosci., vol. 25, no. 9, pages 2312–2321, March 2005. 33, 35, 41, 46

[Benda 2007] Jan Benda and R. Matthias Hennig. *Spike-frequency adaptation generates intensity invariance in a primary auditory interneuron.* Journal of Computational Neuroscience, vol. 24, no. 2, pages 113–136, 2007. 4, 46

[Benda 2010] Jan Benda, Leonard Maler and André Longtin. *Linear Versus Nonlinear Signal Transmission in Neuron Models With Adaptation Currents or Dynamic Thresholds.* Journal of Neurophysiology, vol. 104, no. 5, pages 2806 –2820, November 2010. 2

[Berry 1998] Michael J Berry and Markus Meister. *Refractoriness and Neural Precision.* J. Neurosci, vol. 18, no. 6, pages 2200–2211, March 1998. 6

[Birk 1972] John R. Birk. *Enhanced specificity of information in axons with negatively correlated adjacent interspike intervals.* Kybernetik, vol. 10, no. 4, pages 201–203, 1972. 43

[Borst 2005] Alexander Borst, Virginia L. Flanagin and Haim Sompolinsky. *Adaptation without parameter change: Dynamic gain control in motion detection.* Proceedings of the National Academy of Sciences of the United States of America, vol. 102, no. 17, pages 6172 –6176, April 2005. 46

[Bowden 2001] S. E.H Bowden, S. Fletcher, D. J Loane and N. V Marrion. *Somatic colocalization of rat SK1 and D class (Cav 1.2) L-type calcium channels in rat CA1 hippocampal pyramidal neurons.* Journal of Neuroscience, vol. 21, no. 20, page 175, 2001. 1

[Brandman 2002] R. Brandman and M. E. Nelson. *A Simple Model of Long-Ter m Spike Train Regularization.* Neural Comp., vol. 14, pages 1575–1597, 2002. 17, 44

[Brecht 2004] Michael Brecht, Miriam Schneider, Bert Sakmann and Troy W. Margrie. *Whisker movements evoked by stimulation of single pyramidal cells in rat motor cortex.* Nature, vol. 427, no. 6976, pages 704–710, February 2004. 32

[Bressloff 2009] Paul C. Bressloff. *Stochastic Neural Field Theory and the System-Size Expansion.* SIAM Journal on Applied Mathematics, vol. 70, no. 5, pages 1488–1521, January 2009. 45, 49

[Brockwell 1991] P. J. Brockwell and R. A. Davis. Time series: Theory and methods. Springer, New York, 1991. 10

[Broome 2006] Bede M Broome, Vivek Jayaraman and Gilles Laurent. *Encoding and decoding of overlapping odor sequences.* Neuron, vol. 51, no. 4, pages 467–82, August 2006. 41

[Brown 1980] D. A. Brown and P. R. Adams. *Muscarinic suppression of a novel voltage-sensitive K+ current in a vertebrate neurone.* Nature, vol. 283, no. 5748, pages 673–676, February 1980. 1

[Brown 2001] E. N. Brown, R. Barbieri, Ventura and L. M. Frank. *The Time-Rescaling Theorem and Its Application to Neural Spike Train Data Analysis.* Neural Comp., vol. 14, pages 325–346, 2001. 6

[Brunel 2000] N. Brunel. *Dynamics of sparsely connected networks of excitatory and inhibitory spiking neurons.* Journal of computational neuroscience, vol. 8, no. 3, pages 183–208, 2000. 45, 48

[Buiatti 2003] M. Buiatti and C. van Vreeswijk. *Variance normalisation: a key mechanism for temporal adaptation in natural vision?* Vision research, vol. 43, no. 17, pages 1895–1906, 2003. 47

[Buonocore 2010] A. Buonocore, L. Caputo, E. Pirozzi and L.M. Ricciardi. *On a Stochastic Leaky Integrate-and-Fire Neuronal Model.* Neural Computation, vol. 22, no. 10, pages 2558–2585, 2010. 45

[Burns 1976] B. Delisle Burns and A. C. Webb. *The Spontaneous Activity of Neurones in the Cat's Cerebral Cortex.* In Proceedings of the Royal Society of London. Series B, Biological Sciences, pages 211–233, 1976. 12

[Casagrande 1985] F. Casagrande, L. A. Lugiato and G. Strini. *Adiabatic elimination technique for quantum dissipative systems.* In Luigi Accardi and Wilhelm Waldenfels, editeurs, Quantum Probability and Applications II, volume 1136. Springer Berlin Heidelberg, 1985. 49

[Câteau 2006] Hideyuki Câteau and Alex D Reyes. *Relation between single neuron and population spiking statistics and effects on network activity.* Phys Rev Lett, vol. 96, no. 5, page 058101, February 2006. 27

[Chacron 2000] M. J. Chacron, A. Longtin, M. St-Hilaire and L. Maler. *Suprathreshold Stochastic Firing Dynamics with Memory in $P-type$ electroreceptors.* Phys. Rev. Lett., vol. 85, no. 7, pages 1576–1579, 2000. 6, 7, 17, 19

[Chacron 2001] Maurice J. Chacron, A. Longtin and L. Maler. *Negative interspike interval correlations increase the neuronal capacity for encoding time-dependent stimuli.* J. Neurosci., vol. 21(14), pages 5328–5343, 2001. 17, 29, 44

[Chacron 2004] Maurice J Chacron, Benjamin Lindner and André Longtin. *Noise Shaping by Interval Correlations Increases Information Transfer.* Phys. Rev. Lett., vol. 92, no. 8, page 080601, February 2004. 17, 18, 19, 29

[Chou 2010] Ya-Hui Chou, Maria L Spletter, Emre Yaksi, Jonathan C S Leong, Rachel I Wilson and Liqun Luo. *Diversity and wiring variability of olfactory local interneurons in the Drosophila antennal lobe.* Nature Neuroscience, vol. 13, no. 4, pages 439–449, 2010. 35

[Churchland 2010] Mark M Churchland, Byron M Yu, John P Cunningham, Leo P Sugrue, Marlene R Cohen, Greg S Corrado, William T Newsome, Andrew M Clark, Paymon Hosseini, Benjamin B Scott, David C Bradley, Matthew A Smith, Adam Kohn, J Anthony Movshon, Katherine M Armstrong, Tirin Moore, Steve W Chang, Lawrence H Snyder, Stephen G Lisberger, Nicholas J Priebe, Ian M Finn, David Ferster, Stephen I Ryu, Gopal Santhanam, Maneesh Sahani and Krishna V Shenoy. *Stimulus onset quenches neural variability: a widespread cortical phenomenon.* Nat Neurosci, vol. 13, no. 3, pages 369–378, March 2010. 43

[Clopath 2008] Claudia Clopath, Lorric Ziegler, Eleni Vasilaki, Lars Büsing and Wulfram Gerstner. *Tag-Trigger-Consolidation: A Model of Early and Late Long-Term-Potentiation and Depression.* PLoS Comput Biol, vol. 4, no. 12, page e1000248, December 2008. 47

[Corral 2005] Álvaro Corral. *Time-decreasing hazard and increasing time until the next earthquake.* Physical Review E, vol. 71, no. 1, page 017101, January 2005. 49

[Cortes 2011] J. M Cortes, D. Marinazzo, P. Series, M. W Oram, T. J Sejnowski and M. C. W van Rossum. *The effect of neural adaptation of population coding accuracy.* arXiv:1103.2605, March 2011. 47

[Cox 1962] D. R Cox. Renewal theory. Methuen London:, 1962. 6, 14

[Cox 1966] D. R Cox and P. A. W Lewis. The statistical analysis of series of events. Methuen's Monographs on Applied Probability and Statistics. Methuen, London, 1966. 14, 15, 27

[Cox 1970] David R. Cox. Renewal theory. Methuen & Co., 1 édition, June 1970. 2

[Cox 1980] D.R. Cox and Valerie Isham. Point processes. Chapman and Hall/CRC, 1 édition, July 1980. 27

[Dayan 2001] P. Dayan and L. F Abbott. Theoretical neuroscience: Computational and mathematical modeling of neural systems, volume 39. MIT press Cambridge, MA:, 2001. 3

[de Kamps 2003] Marc de Kamps. *A Simple and Stable Numerical Solution for the Population Density Equation.* Neural Computation, vol. 15, no. 9, pages 2129–2146, 2003. 25

[Delgutte 1998] B. Delgutte, B. Hammond and P. Cariani. Psychophysical and physiological advances in hearing, chapter neural coding of the temporal envelope of speech: Relation to modulation transfer functions. Whurr Publishers, Ltd, 1998. 46

[Demmer 2009] Heike Demmer and Peter Kloppenburg. *Intrinsic Membrane Properties and Inhibitory Synaptic Input of Kenyon Cells as Mechanisms for Sparse Coding?* J Neurophysiol, vol. 102, no. 3, pages 1538–1550, September 2009. 33, 47

[Destexhe 2003] A. Destexhe, M. Rudolph and D. Pare. *The high-conductance state of neocortical neurons in vivo.* Nat Rev Neurosci, vol. 4, no. 9, pages 739–751, 2003. 43

[Devroye 1986] Luc Devroye. Non-uniform random variate generation. Springer-Verlag, New York, 1986. 6

[DeWeese 2003] Michael R. DeWeese, Michael Wehr and Anthony M. Zador. *Binary Spiking in Auditory Cortex.* The Journal of Neuroscience, vol. 23, no. 21, pages 7940 –7949, 2003. 32

[Diesmann 1999] Markus Diesmann, Marc-Oliver Gewaltig and Ad Aertsen. *Stable propagation of synchronous spiking in cortical neural networks.* Nature, vol. 402, no. 6761, pages 529–533, December 1999. 47

[Ellis 2007] Lee D. Ellis, W. Hamish Mehaffey, Erik Harvey-Girard, Ray W. Turner, Leonard Maler and Robert J. Dunn. *SK Channels Provide a Novel Mechanism for the Control of Frequency Tuning in Electrosensory Neurons.* The Journal of Neuroscience, vol. 27, no. 35, pages 9491 –9502, 2007. 47

[Engel 2008] T.A. Engel, L. Schimansky-Geier, A.V.M. Herz, S. Schreiber and I. Erchova. *Membrane potential resonances shape spontaneous firing patterns in the entorhinal cortex.* J Neurophysiol., vol. In press, 2008. 7, 17

[Eppler 2008] Jochen Martin Eppler, Moritz Helias, Eilif Muller, Markus Diesmann and Marc-Oliver Gewaltig. *PyNEST: A Convenient Interface to the NEST Simulator.* Frontiers in Neuroinformatics, vol. 2, 2008. PMID: 19198667 PMCID: 2636900. 35, 51

[Ermentrout 2001] Bard Ermentrout, Matthew Pascal and Boris Gutkin. *The Effects of Spike Frequency Adaptation and Negative Feedback on the Synchronization of Neural Oscillators.* Neural Computation, vol. 13, no. 6, pages 1285–1310, 2001. 1

[Fano 1947] U. Fano. *Ionization Yield of Radiations. II. The Fluctuations of the Number of Ions.* Physical Review, vol. 72, no. 1, page 26, July 1947. 2, 14

[Farkhooi 2008] Farzad Farkhooi, Clemens Boucsein and Martin Nawrot. *Negative serial dependence between spiking intervals improve rate estimation in postsynaptic cortical ensemble.* In AREADNE 2008 - Research in Encoding And Decoding of Neural Ensembles, Santorini, Greece, June 2008. 19

[Farkhooi 2009a] Farzad Farkhooi, Eilif Muller and Martin Nawrot. *Sequential sparsing by successive adapting neural populations.* BMC Neuroscience, vol. 10, no. Suppl 1, page O10, 2009. iii

[Farkhooi 2009b] Farzad Farkhooi, Martin F. Strube-Bloss and Martin P. Nawrot. *Serial correlation in neural spike trains: Experimental evidence, stochastic modeling, and single neuron variability.* Physical Review E, vol. 79, no. 2, page 021905, February 2009. iii, 2, 24, 28

[Farkhooi 2010] Farzad Farkhooi, Eilif Muller and Martin P Nawrot. *Sequential Sparsening by Successive Adaptation in Neural Populations.* arXiv:1007.2345, July 2010. Supplement to Farkhooi, F., Muller, E. & Nawrot, M. Sequential sparsing by successive adapting neural populations. BMC Neuroscience 10, O10 (2009). iii

[Farkhooi 2011a] Farzad Farkhooi, Eilif Muller and Martin P. Nawrot. *Adaptation reduces variability of the neuronal population code.* Phys. Rev. E, vol. 83, page 050905, May 2011. iii

[Farkhooi 2011b] Farzad Farkhooi, Eilif Muller and Martin P Nawrot. *Adaptation Reduces Variability of the Neuronal Population Code.* arXiv:1007.3490v2, 2011. iii, 38, 42

[Fiete 2004] Ila R. Fiete, Richard H.R. Hahnloser, Michale S. Fee and H. Sebastian Seung. *Temporal Sparseness of the Premotor Drive Is Important for Rapid Learning in a Neural Network Model of Birdsong.* Journal of Neurophysiology, vol. 92, no. 4, pages 2274 –2282, October 2004. 32

[Fleidervish 1996] I. A Fleidervish, A. Friedman and M. J. Gutnick. *Slow inactivation of Na+ current and slow cumulative spike adaptation in mouse and guinea-pig neocortical neurones in slices.* The Journal of Physiology, vol. 493, no. Pt 1, page 83, 1996. 1

[Floyd 1982] K. Floyd, V. H. Hick, A.V. Holden, J. Koley and J.F. B. Morrison. *Non-Markov Negative Correlation Between Interspike Intervals in Mammalian Sympathetic Efferent Discharges.* Biol. Cybern., vol. 45, pages 89–93, 1982. 7

[Földiák 1995] P. Földiák and M. P. Young. The handbook of brain theory and neural networks, chapter sparse coding in the primate cortex. MIT Press, Cambridge, 1995. 32

[French 2001] Andrew S. French, Ulli Hüger, Shinichi Sekizawa and Päivi H. Torkkeli. *Frequency response functions and information capacities of paired spider mechanoreceptor neurons.* Biological Cybernetics, vol. 85, no. 4, pages 293–300, 2001. 46

[Froese 2009] Anja Froese. *Olfactory processing in honeybee Kenyon cells and the involvement of the GABAergic system.* PhD thesis, FU Berlin, Berlin, 2009. 38

[Fuhrmann 2002] Galit Fuhrmann, Henry Markram and Misha Tsodyks. *Spike Frequency Adaptation and Neocortical Rhythms.* Journal of Neurophysiology, vol. 88, no. 2, pages 761 –770, 2002. 1, 42

[Fuwape 2008] Ibiyinka Fuwape and Alexander B. Neiman. *Spontaneous firing statistics and information transfer in electroreceptors of paddlefish.* Physical Review E, vol. 78, no. 5, page 051922, November 2008. 29

[Gardiner 1984] C. W. Gardiner. *Adiabatic elimination in stochastic systems. I. Formulation of methods and application to few-variable systems.* Physical Review A, vol. 29, no. 5, page 2814, May 1984. 48

[Gardiner 2004] Crispin Gardiner. Handbook of stochastic methods: for physics, chemistry and the natural sciences. Springer, 3rd édition, April 2004. 3, 25, 48

[Gaver 1980] D. P Gaver and P. A. W Lewis. *First-Order Autoregressive Gamma Sequences and Point Processes.* Advances in Applied Probability, vol. 12, no. 3, pages 727–745, 1980. 17

[Geffen 2009] Maria N. Geffen, Bede M. Broome, Gilles Laurent and Markus Meister. *Neural Encoding of Rapidly Fluctuating Odors.* Neuron, vol. 61, no. 4, pages 570–586, February 2009. 41

[Gerstein 1964] G. L. Gerstein and B. Mandelbrot. *Random walk models for the spike activity of a single neuron.* Biophys. J., vol. 4, pages 41–68, 1964. 5, 12

[Gerstner 1996] W. Gerstner, R. Kempter, J. L Van Hemmen and H. Wagner. *A neuronal learning rule for sub-millisecond temporal coding.* Nature, vol. 383, no. 6595, pages 76–78, 1996. 47

[Gerstner 2002] Wulfram Gerstner and Werner M. Kistler. Spiking neuron models. Cambridge University Press, 1 édition, August 2002. 25

[Gewaltig 2007] Marc-Oliver Gewaltig and Markus Diesmann. *NEST (NEural Simulation Tool).* Scholarpedia, vol. 2, no. 4, page 1430, 2007. 35

[Goense 2003] J. B. M. Goense and R. Ratnam. *Continuous detection of weak sensory signals in afferent spike trains: the role of anti-correlated interspike intervals in detection performance.* Journal of Comparative Physiology A: Sensory, Neural, and Behavioral Physiology, vol. 189, no. 10, pages 741–759, 2003. 44

[Goldberg 2005] Joshua A. Goldberg and Charles J. Wilson. *Control of Spontaneous Firing Patterns by the Selective Coupling of Calcium Currents to Calcium-Activated Potassium Currents in Striatal Cholinergic Interneurons.* The Journal of Neuroscience, vol. 25, no. 44, pages 10230 –10238, November 2005. 1

[Granger 1976] C. W. J. Granger and P. Newbold. *Forecasting Transformed Series.* Journal of the Royal Statistical Society, vol. 38(2), pages 189–203, 1976. 11

[Grunewald 2003] Bernd Grunewald. *Differential expression of voltage-sensitive K+ and Ca2+ currents in neurons of the honeybee olfactory pathway.* J Exp Biol, vol. 206, no. 1, pages 117–129, January 2003. 33, 47

[Haehnel 2009] Melanie Haehnel, Anja Froese and Randolf Menzel. *Invivo Ca2+ Imaging of Mushroom Body Neurons During Olfactory Learning in the Honey Bee.* Journal of Visualized Experiments, no. 30, 2009. 33, 34

[Hartigan 1985] J. A. Hartigan and P. M. Hartigan. *The Dip Test of Unimodality.* The Annals of Statistics, vol. 13, no. 1, pages 70–84, 1985. 14

[Herz 2006] Andreas V M Herz, Tim Gollisch, Christian K Machens and Dieter Jaeger. *Modeling single-neuron dynamics and computations: a balance of detail and abstraction.* Science, vol. 314, no. 5796, pages 80–85, October 2006. 16, 17

[Herz 2008] A. V.M Herz, R. Meier, M. P Nawrot, W. Schiegel and T. Zito. *G-Node: An integrated tool-sharing platform to support cellular and systems neurophysiology in the age of global neuroinformatics.* Neural Networks, vol. 21, no. 8, pages 1070–1075, 2008. 20

[Hromádka 2008] T. Hromádka, M. R DeWeese and A. M. Zador. *Sparse Representation of Sounds in the Unanesthetized Auditory Cortex.* PLoS Biol, vol. 6, no. 1, page e16, January 2008. 32

[Ito 2008] Iori Ito, Rose Chik-Ying Ong, Baranidharan Raman and Mark Stopfer. *Sparse odor representation and olfactory learning.* Nat Neurosci, vol. 11, no. 10, pages 1177–84, October 2008. 33, 35, 41, 46

[Jann 1996] A. Jann and Y. Ben-Aryeh. *Quantum-noise reduction in semiconductor lasers.* Journal of the Optical Society of America B, vol. 13, no. 5, pages 761–767, May 1996. 50

[Johnson 1996] D. H. Johnson. *Point Process Model of Single-Neuron Discharges.* J. of Comp. Neurosci., vol. 3, no. 4, pages 275–299, 1996. 5, 6, 18

[Johnston 1954] J. Johnston and J. Dinardo. Econometric methods. McGraw-Hilll, Singapore, 1954. 8, 13

[Jortner 2007] Ron A Jortner, S Sarah Farivar and Gilles Laurent. *A simple connectivity scheme for sparse coding in an olfactory system.* J Neurosci, vol. 27, no. 7, pages 1659–69, February 2007. 33, 35

[Joshua 2007] M. Joshua, S. Elias, O. Levine and H. Bergman. *Quantifying the isolation quality of extracellularly recorded action potentials.* J. Neurosci. Meth., vol. 163, pages 267–282, 2007. 15

[Kaissling 1987] K.-E. Kaissling, C. Zack Strausfeld and E. R. Rumbo. *Adaptation Processes in Insect Olfactory Receptors.* Annals of the New York Academy of Sciences, vol. 510, no. 1 Olfaction and, pages 104–112, 1987. 33, 41

[Kampen 2007] N. G. Van Kampen. Stochastic processes in physics and chemistry. Elsevier Science & Technology, 0003 édition, March 2007. 18

[Kass 2001] Robert E Kass and Valerie Ventura. *A Spike-Train Probability Model.* Neural Comp., vol. 13, no. 8, pages 1713–1720, 2001. 6

[Katz 2010] Yuri A. Katz and Nikolai V. Shokhirev. *Default risk modeling beyond the first-passage approximation: Extended Black-Cox model.* Physical Review E, vol. 82, no. 1, page 016116, July 2010. 49

[Kazama 2008] Hokto Kazama and Rachel I. Wilson. *Homeostatic Matching and Nonlinear Amplification at Identified Central Synapses.* Neuron, vol. 58, no. 3, pages 401–413, May 2008. 33, 41

[Kendall 1962] M.G. Kendall. Rank correlation methods. Griffin, London, 1962. 10, 18

[Krofczik 2008] Sabine Krofczik. *Rapid odor processing in the honeybee antennal lobe network.* Frontiers in Computational Neuroscience, vol. 2, 2008. 35, 41

[Kuffler 1957] S. W. Kuffler, R. Fitzhugh and H. B. Barlow. *Maintained Activity in the cat's retina in light and darkness.* J. Gen. Physiol., vol. 50, no. 5, pages 683–702, 1957. 6, 7, 12

[Kumar 2010] Arvind Kumar, Stefan Rotter and Ad Aertsen. *Spiking activity propagation in neuronal networks: reconciling different perspectives on neural coding.* Nat Rev Neurosci, vol. 11, no. 9, pages 615–627, 2010. 47

[LaCamera 2004] Giancarlo LaCamera, Alexander Rauch, Hans-R Luscher, Walter Senn and Stefano Fusi. *Minimal models of adapted neuronal response to in vivo-like input currents.* Neural Comput, vol. 16, no. 10, pages 2101–2124, October 2004. 48

[Latham 2000] P. E. Latham, B. J. Richmond, P. G. Nelson and S. Nirenberg. *Intrinsic Dynamics in Neuronal Networks. I. Theory.* J Neurophysiol, vol. 83, no. 2, pages 808–827, February 2000. 42

[Laughlin 1981] S. Laughlin. *A simple coding procedure enhances a neuron's information capacity.* Z. Naturforsch, vol. 36, no. 9-10, pages 910–912, 1981. 43, 44

[Laurent 1999] Gilles Laurent. *A Systems Perspective on Early Olfactory Coding.* Science, vol. 286, no. 5440, pages 723 –728, October 1999. 42

[Laurent 2002] Gilles Laurent. *Olfactory network dynamics and the coding of multidimensional signals.* Nat Rev Neurosci, vol. 3, no. 11, pages 884–895, November 2002. 33, 47

[Lawrence 1973] A. J. Lawrence. *Dependency of Intervals Between Events in Superposition Processes.* Journal of the Royal Statistical Society. Series B (Methodological), vol. 35, no. 2, pages 306–315, 1973. 27

[Lehmann 1953] E. L. Lehmann. *The Power of Rank Test.* Annals Math. Stat., vol. 24, no. 1, pages 23–43, 1953. 18

[Leopold 2003] D. A Leopold, Y. Murayama and N. K Logothetis. *Very slow activity fluctuations in monkey visual cortex: implications for functional brain imaging.* Cerebral Cortex, vol. 4, no. 13, pages 422–433, April 2003. 19

[Levine 1980] M. W. Levine. *Point Process Model of Single-Neuron Discharges.* Biophysical J., vol. 30, pages 9–26, 1980. 6, 7

[Levine 1991] M. W. Levine. *The Distribution of the intervals between neural impulses in maintained discharges of retinal ganglion cell.* Biol. Cybern., vol. 65, pages 459–467, 1991. 12

[Lewicki 2002] Michael S. Lewicki. *Efficient coding of natural sounds.* Nat Neurosci, vol. 5, no. 4, pages 356–363, April 2002. 46

[Lindner 2006] Benjamin Lindner. *Superposition of many independent spike trains is generally not a Poisson process.* Physical Review E, vol. 73, no. 2, page 022901, February 2006. 27

[Lindner 2007] Benjamin Lindner and Tilo Schwalger. *Correlations in the Sequence of Residence Times.* Physical Review Letters, vol. 98, no. 21, page 210603, May 2007. 24

[Lindner 2009] Benjamin Lindner, Dorian Gangloff, André Longtin and John E. Lewis. *Broadband Coding with Dynamic Synapses.* The Journal of Neuroscience, vol. 29, no. 7, pages 2076 –2087, February 2009. 47

[Liu 2001] Y H Liu and X J Wang. *Spike-frequency adaptation of a generalized leaky integrate-and-fire model neuron.* J Comput Neurosci, vol. 10, no. 1, pages 25–45, 2001. 2, 16, 17, 24

[Livina 2005] Valerie N. Livina, Shlomo Havlin and Armin Bunde. *Memory in the Occurrence of Earthquakes.* Physical Review Letters, vol. 95, no. 20, page 208501, November 2005. 24, 51

[London 2010] Michael London, Arnd Roth, Lisa Beeren, Michael Hausser and Peter E. Latham. *Sensitivity to perturbations in vivo implies high noise and suggests rate coding in cortex.* Nature, vol. 466, no. 7302, pages 123–127, July 2010. 43

[Longtin 2003] A. Longtin and MJ Chacron. *Correlations and Memory in Neurodynamical Systems.* In Govindan Rangarajan and Mingzhou Ding, editeurs, Processes with Long-Range Correlations, volume 621. Springer Berlin Heidelberg, Berlin, Heidelberg, 2003. 17, 44

[Lüdtke 2006] N. Lüdtke and M. E Nelson. *Short-term synaptic plasticity can enhance weak signal detectability in nonrenewal spike trains.* Neural computation, vol. 18, no. 12, pages 2879–2916, 2006. 17, 19

[Lundstrom 2008] Brian N Lundstrom, Matthew H Higgs, William J Spain and Adrienne L Fairhall. *Fractional differentiation by neocortical pyramidal neurons*. Nat Neurosci, vol. 11, no. 11, pages 1335–42, November 2008. 30, 41, 42, 46

[MacLeod 1996] Katrina MacLeod and Gilles Laurent. *Distinct Mechanisms for Synchronization and Temporal Patterning of Odor-Encoding Neural Assemblies*. Science, vol. 274, no. 5289, pages 976 –979, November 1996. 42

[Madison 1984] D V Madison and R A Nicoll. *Control of the repetitive discharge of rat CA 1 pyramidal neurones in vitro.* The Journal of Physiology, vol. 354, no. 1, pages 319 –331, 1984. 1

[Mar 1999] D. J. Mar, C. C. Chow, W. Gerstner, R. W. Adams and J. J. Collins. *Noise shaping in populations of coupled model neurons*. Proceedings of the National Academy of Sciences of the United States of America, vol. 96, no. 18, pages 10450–10455, 1999. 42, 44

[Mattia 2002] Maurizio Mattia and Paolo Del Giudice. *Population dynamics of interacting spiking neurons*. Physical Review E, vol. 66, no. 5, page 051917, November 2002. 49

[Mazor 2005] Ofer Mazor and Gilles Laurent. *Transient Dynamics versus Fixed Points in Odor Representations by Locust Antennal Lobe Projection Neurons*. Neuron, vol. 48, no. 4, pages 661–673, November 2005. 42

[McCormick 1989] D. A. McCormick and A. Williamson. *Convergence and divergence of neurotransmitter action in human cerebral cortex.* Proc. Natl. Acad. Sci., vol. 86, pages 8098–8102, 1989. 16

[McFadden 1962] J. A McFadden. *On the Lengths of Intervals in a Stationary Point Process.* Journal of the Royal Statistical Society. Series B (Methodological), vol. 24, no. 2, pages 364–382, 1962. 26, 27, 50

[Mehaffey 2008] W. Hamish Mehaffey, Lee D. Ellis, Rüdiger Krahe, Robert J. Dunn and Maurice J. Chacron. *Ionic and neuromodulatory regulation of burst discharge controls frequency tuning.* Journal of Physiology-Paris, vol. 102, no. 4-6, pages 195–208, 2008. 47

[Meier 2008] R. Meier, U. Egert, A. Aertsen and M. P. Nawrot. *FIND - A unified framework for neural data analysis.* Neural Networks, vol. in press, 2008. doi:10.1016/j.neunet.2008.06.019. 20

[Menzel 2001] R. Menzel. *Searching for the Memory Trace in a Mini-Brain, the Honeybee.* Learning and Memory, vol. 8, no. 2, pages 53–62, 2001. 7

[Menzel 2009] R. Menzel and Larry R. Squire. *Olfaction in Invertebrates: Honeybee.* In Encyclopedia of Neuroscience, pages 43–48. Academic Press, Oxford, 2009. 35, 37

[Mercer 2002] Alison R. Mercer and John G. Hildebrand. *Developmental Changes in the Density of Ionic Currents in Antennal-Lobe Neurons of the Sphinx Moth, Manduca sexta.* J Neurophysiol, vol. 87, no. 6, pages 2664–2675, June 2002. 33, 47

[Merkel 2010] Matthias Merkel and Benjamin Lindner. *Synaptic filtering of rate-coded information.* Physical Review E, vol. 81, no. 4, page 041921, April 2010. 33

[Moore 1966] G. O. Moore, D. Perkel and Jose Segundo. *Statistical Analysis and Functional Interpretation of Neuronal Spike Data.* Annu. Rev. Physiol., vol. 28, pages 493–522, 1966. 2, 5, 43

[Moreno-Bote 2008] Rubén Moreno-Bote, Alfonso Renart and Néstor Parga. *Theory of input spike auto- and cross-correlations and their effect on the response of spiking neurons.* Neural Comput, vol. 20, no. 7, pages 1651–705, July 2008. 29

[Moreno 2002] Rubén Moreno, Jaime de la Rocha, Alfonso Renart and Néstor Parga. *Response of Spiking Neurons to Correlated Inputs.* Physical Review Letters, vol. 89, no. 28, page 288101, December 2002. 29

[Muller 2007] Eilif Muller, Lars Buesing, Johannes Schemmel and Karlheinz Meier. *Spike-Frequency Adapting Neural Ensembles: Beyond Mean Adaptation and Renewal Theories.* Neural Comp., vol. 19, no. 11, pages 2958–3010, 2007. 2, 3, 17, 25, 26, 27, 28, 30, 34, 37, 38, 45, 47, 48, 50, 51

[Nagel 2011] Katherine I Nagel and Rachel I Wilson. *Biophysical mechanisms underlying olfactory receptor neuron dynamics.* Nature Neuroscience, vol. 14, no. 2, pages 208–216, 2011. 33, 35, 41

[Namiki 2008] Shigehiro Namiki and Ryohei Kanzaki. *Reconstructing the population activity of olfactory output neurons that innervate identifiable processing units.* Frontiers in Neural Circuits, vol. 2, 2008. 41

[Nawrot 2003] Martin P Nawrot. *Ongoing activity in cortical networks: noise, variability and context.* PhD thesis, Faculty of Biology, Albert-Ludwigs-University Freiburg, Germany, June 2003. 19

[Nawrot 2007] M. P. Nawrot, C. Boucsein, V. Rodriguez-Molina, Ad Aertsen, Sonja Grün and Stefan Rotter. *Serial interval statistics of spontaneous activity in cortical neurons in vivo and in vitro.* Neurocomputing, vol. 70, pages 1717–1722, 2007. doi:10.1016/j.neucom.2006.10.101. 7, 19, 23, 28, 44

[Nawrot 2008] M. P. Nawrot, C. Boucsein, V. R. Molina, A. Riehle, A. Aertsen and S. Rotter. *Measurement of variability dynamics in cortical spike trains.* J Neurosci. Methods, vol. 169, no. 2, pages 374–390, April 2008. 2, 6, 14, 19, 23, 43

[Nawrot 2010a] Martin P. Nawrot. *Analysis and Interpretation of Interval and Count Variability in Neural Spike Trains.* In Sonja Grün and Stefan Rotter, editeurs, Analysis of Parallel Spike Trains. Springer US, Boston, MA, 2010. 43

[Nawrot 2010b] Martin Paul Nawrot, Sabine Krofczik, Farzad Farkhooi and Randolf Menzel. *Fast dynamics of odor rate coding in the insect antennal lobe.* arXiv:1101.0271, December 2010. 37, 41

[Neiman 2001] A. Neiman and D. F. Russell. *Stochastic Biperiodic Oscillations in the Electroreceptors of Paddlefish.* Physical Rev. Lett., vol. 86, pages 3443–3446, 2001. 16

[Neiman 2004] A. B. Neiman and D. F. Russell. *Two Distinct Types of Noisy Oscillators in Electroreceptors of Paddlefish.* J. Neurophysiol., vol. 92, pages 492–509, 2004. 6, 7, 16, 19

[Neiman 2005] Alexander B Neiman and David F Russell. *Models of stochastic biperiodic oscillations and extended serial correlations in electroreceptors of paddlefish.* Physical Rev. E, vol. 71, pages 061915–1–061915–10, 2005. 16

[Nelson 1997] M. E. Nelson, Z. Xu and J. R. Payne. *Characterization and modeling of P-type electrosensory afferent responses to amplitude modulations in a wave-type electric fish.* Journal of Comparative Physiology A: Sensory, Neural, and Behavioral Physiology, vol. 181, no. 5, pages 532–544, 1997. 46

[Nemenman 2008] Ilya Nemenman, Geoffrey D. Lewen, William Bialek and Rob R. de Ruyter van Steveninck. *Neural Coding of Natural Stimuli: Information at Sub-Millisecond Resolution.* PLoS Comput Biol, vol. 4, no. 3, page e1000025, March 2008. 43

[Nemenman 2010] Ilya Nemenman. *Information theory and adaptation.* arXiv:1011.5466, November 2010. To appear as Chapter 5 of Quantitative Biology: From Molecular to Cellular Systems, ME Wall, ed. (Taylor and Francis, 2011). 43, 47

[Nesse 2008] William H. Nesse, Christopher A. Del Negro and Paul C. Bressloff. *Oscillation Regularity in Noise-Driven Excitable Systems with Multi-Time-Scale Adaptation.* Physical Review Letters, vol. 101, no. 8, page 088101, 2008. 48

[Nesse 2010] William H. Nesse, Leonard Maler and André Longtin. *Biophysical information representation in temporally correlated spike trains.* Proceedings of the National Academy of Sciences, vol. 107, no. 51, pages 21973 –21978, December 2010. 44, 45

[Okada 2007] J. Rybak R. Okada and R. Menzel. *Learning-Related Plasticity in PE1 and Other Mushroom Body-Extrinsic Neurons in the Honeybee Brain.* J. of Neurosci., vol. 27, no. 43, pages 11736–11747, 2007. 7

[Olshausen 1996] B. A Olshausen*et al.* *Emergence of simple-cell receptive field properties by learning a sparse code for natural images.* Nature, vol. 381, no. 6583, pages 607–609, 1996. 46

[Olshausen 2004] Bruno A Olshausen and David J Field. *Sparse coding of sensory inputs.* Current Opinion in Neurobiology, vol. 14, no. 4, pages 481–487, August 2004. 32, 33, 46

[Ortega 2003] E.M.M. Ortega, H. Bolfarine and G.A. Paula. *Influence diagnostics in generalized log-gamma regression models.* Computational Statistics and Data Analysis, vol. 42, no. 22, pages 165–186, 2003. 13

[Palm 1980] G. Palm. *On associative memory.* Biological Cybernetics, vol. 36, no. 1, pages 19–31, 1980. 32

[Pennefather 1985] P. Pennefather, B. Lancater, P. R. Adams and R. A. Nicoll. *Two distinct Ca-dependent K currents in bullfrog sympathetic ganglion cells.* Proc. Natl. Acad. Sci., vol. 82, pages 3040–3044, 1985. 16

[Perez-Orive 2002] Javier Perez-Orive, Ofer Mazor, Glenn C. Turner, Stijn Cassenaer, Rachel I. Wilson and Gilles Laurent. *Oscillations and Sparsening of Odor Representations in the Mushroom Body.* Science, vol. 297, no. 5580, pages 359 –365, July 2002. 4, 32, 33, 46

[Perkel 1967a] D. H. Perkel, G. L. Gerstein and G. Moore. *Neuronal Spike Trains and Stochastic Point Processes: I The single Spike Train.* Biophysical J., vol. 7, pages 391–418, 1967. 2, 5, 6, 8, 12, 43

[Perkel 1967b] D. H. Perkel, G. L. Gerstein and G. Moore. *Neuronal Spike Trains and Stochastic Point Processes: II Simulation Spike Train.* Biophysical J., vol. 7, pages 419–440, 1967. 2, 5, 6, 43

[Peron 2009] Simon Peron and Fabrizio Gabbiani. *Spike frequency adaptation mediates looming stimulus selectivity in a collision-detecting neuron.* Nat Neurosci, vol. 12, no. 3, pages 318–326, March 2009. 47

[Phillips 1988] P. C. B. Phillips and P. Perron. *Testing for a unit root in time series regression.* Biometrika, vol. 75, no. 2, pages 335–346, 1988. 8

[Poo 2009] Cindy Poo and Jeffry S. Isaacson. *Odor Representations in Olfactory Cortex: "Sparse" Coding, Global Inhibition, and Oscillations.* Neuron, vol. 62, no. 6, pages 850–861, June 2009. 32

[Pouzat 2004] C. Pouzat, M. Delescluse, P. Viot and J. Diebolt. *Improved spike-sorting by modeling firing statistics and burst-dependent spike amplitude attenuation: a Markov chain Monte Carlo approach.* J. Neurophysiol, vol. 91, pages 2910–1928, 2004. 15

[Prescott 2008] Steven A Prescott and Terrence J Sejnowski. *Spike-rate coding and spike-time coding are affected oppositely by different adaptation mechanisms.* J Neurosci, vol. 28, no. 50, pages 13649–61, December 2008. 44

[Press 1992] William H Press, Saul A Teukolsky, William T Vetterling and Brian P Flannery. Numerical recipes in c. Cambridge University Press, 2 édition, 1992. 18

[Ratnam 2000] Rama Ratnam and Mark E. Nelson. *Nonrenewal Statistics of Electrosensory Afferent Spike Trains: Implications for the Detection of Weak Sensory Signals.* J. Neurosci., vol. 20, no. 17, pages 6672–6683, September 2000. 6, 7, 19, 28, 44

[Reich 1998] D. S. Reich, J. D. Victor and B. W. Knight. *The Power Ratio and the Interval Map: Spiking Models and Extracellular Recordings.* J. of Neurosci., vol. 18, no. 23, pages 10098–10104, 1998. 6

[Rodieck 1967] R. W. Rodieck. *Maintained activity of cat retinal ganglion cells.* J. of Neurophysiol., vol. 50, no. 5, pages 1044–1071, 1967. 6, 7

[Rotter 2005] Stefan Rotter, Alexa Riehle, Victor Rodriguez-Molina, Ad Aertsen and Martin P Nawrot. *Different time scales of spike train variability in motor cortex.* In Soc. Neurosci. Abstr. Online, page 276.7, 2005. 19

[Sachse 2002] Silke Sachse and C. Giovanni Galizia. *Role of Inhibition for Temporal and Spatial Odor Representation in Olfactory Output Neurons: A Calcium Imaging Study.* J Neurophysiol, vol. 87, no. 2, pages 1106–1117, February 2002. 34, 35, 37

[Saleh 1987] B. E. A. Saleh and M. C. Teich. *Can the channel capacity of a light-wave communication system be increased by the use of photon-number squeezed light?* Physical Review Letters, vol. 58, no. 25, page 2656, June 1987. 50

[Sanchez-Vives 2000a] M V. Sanchez-Vives, L. G. Nowak and D. A. McCormick. *Cellular Mechanisms of Long-Lasting Adaptation in Visual Cor tical Neurons In Vitro.* The Journal of Neuroscience, vol. 20, no. 11, pages 4286–4299, 2000. 16

[Sanchez-Vives 2000b] Maria V. Sanchez-Vives, Lionel G. Nowak and David A. McCormick. *Membrane Mechanisms Underlying Contrast Adaptation in Cat Area 17In Vivo.* The Journal of Neuroscience, vol. 20, no. 11, pages 4267 –4285, June 2000. 1

[Schafer 1994] S Schafer, H Rosenboom and R Menzel. *Ionic currents of Kenyon cells from the mushroom body of the honeybee.* J. Neurosci., vol. 14, no. 8, pages 4600–4612, August 1994. 33, 47

[Schwindt 1988] P. C. Schwindt, W. J. Spain, R. C. Foehring, C. E. Stafstrom, M. C. Chubb and W. E. Crill. *Multiple potassium conductances and their functions* *in neurons from cat sensorimotor cortex in vitro.* Journal of neurophysiology, vol. 59, no. 2, page 424, 1988. 1

[Schwindt 1989] P. C. Schwindt, W. J. Spain and W. E. Crill. *Long-lasting reduction of excitability by a sodium-dependent potassium current in cat neocortical neurons.* Journal of neurophysiology, vol. 61, no. 2, page 233, 1989. 1

[Shadlen 1998] Michael N Shadlen and William T Newsome. *The Variable Discharge of Cortical Neurons: Implications for Connectivity, Computation, and Information Coding.* J. Neurosci., vol. 18, no. 10, pages 3870–3896, 1998. 2, 43, 47

[Siegert 1951] Arnold J. F. Siegert. *On the First Passage Time Probability Problem.* Physical Review, vol. 81, no. 4, page 617, February 1951. 45, 48

[Sivan 2006] Ehud Sivan and Nancy Kopell. *Oscillations and slow patterning in the antennal lobe.* Journal of Computational Neuroscience, vol. 20, no. 1, pages 85–96, 2006. 41

[Sobel 1994] E. C Sobel and D. W Tank. *In vivo Ca2+ dynamics in a cricket auditory neuron: an example of chemical computation.* Science, vol. 263, no. 5148, page 823, 1994. 1

[Soler 2008] Felipe Caycedo Soler, Ferney J. Rodriguez and Gert Zumofen. *Memory in the photon statistics of multilevel quantum systems.* Physical Review A, vol. 78, no. 5, page 053813, November 2008. 24, 50

[Song 2000] Sen Song, Kenneth D. Miller and L. F. Abbott. *Competitive Hebbian learning through spike-timing-dependent synaptic plasticity.* Nat Neurosci, vol. 3, no. 9, pages 919–926, 2000. 47

[Stein 1965] R. B. Stein. *Some Models of Neuronal Variability.* Biophys. J, vol. 7, no. 1, pages 37–68, 1965. 5, 6, 12

[Stein 2005] Richard B. Stein, E. Roderich Gossen and Kelvin E. Jones. *Neuronal variability: noise or part of the signal?* Nat Rev Neurosci, vol. 6, no. 5, pages 389–397, May 2005. 43

[Storm 1990] Johan F. Storm, J. Zimmer and O.P. Ottersen J. Storm-Mathisen. *Chapter 12 Potassium currents in hippocampal pyramidal cells.* In Understanding the Brain Through the Hippocampus the Hippocampal Region as a Model for Studying Brain Structure and Function, volume Volume 83, pages 161–187. Elsevier, 1990. 1

[Strube-Bloss 2008] M. F. Strube-Bloss. *Characterization of Mushroom Body Extrinsic Neurons of the Honeybee: Oder Specificity, Response Reliablity and Learning Related Plasticity.* PhD thesis, Neurobiology, Department of Biology, Chemistry, and Pharmacy, Free University of Berlin, 2008. 7

[Szyszka 2005] Paul Szyszka, Mathias Ditzen, Alexander Galkin, C. Giovanni Galizia and Randolf Menzel. *Sparsening and Temporal Sharpening of Olfactory Representations in the Honeybee Mushroom Bodies.* Journal of Neurophysiology, vol. 94, no. 5, pages 3303 –3313, November 2005. 33, 34, 35, 37, 41, 46

[Tolhurst 2009] David J. Tolhurst, Darragh Smyth and Ian D. Thompson. *The Sparseness of Neuronal Responses in Ferret Primary Visual Cortex.* The Journal of Neuroscience, vol. 29, no. 8, pages 2355 –2370, February 2009. 32

[Trapletti 2011] Adrian Trapletti and Kurt Hornik. *tseries: Time Series Analysis and Computational Finance*, 2011. R package version 0.10-25. 8

[Tripp 2009] Bryan Tripp and Chris Eliasmith. *Population Models of Temporal Differentiation.* Neural Computation, November 2009. PMID: 19922294. 41, 42, 46

[Truccolo 2005] Wilson Truccolo, Uri T. Eden, Matthew R. Fellows, John P. Donoghue and Emery N. Brown. *A Point Process Framework for Relating Neural Spiking Activity to Spiking History, Neural Ensemble, and Extrinsic Covariate Effects.* J Neurophysiol, vol. 93, no. 2, pages 1074–1089, February 2005. 18

[Tsodyks 1998] Misha Tsodyks, Klaus Pawelzik and Henry Markram. *Neural Networks with Dynamic Synapses.* Neural Computation, vol. 10, no. 4, pages 821–835, 1998. 35

[Tsuchitani 1985] C. Tsuchitani and D H Johnson. *The effects of ipsilateral tone-burst stimlus level on the discharge patterns of cat lateral superior olivary units.* JASA, vol. 77, pages 1484–1496, 1985. 6, 7, 16

[Tuckwell 2005] Henry C. Tuckwell. Introduction to theoretical neurobiology: Volume 2, nonlinear and stochastic theories. Cambridge University Press, September 2005. 5, 6, 12, 14

[Turner 2008] Glenn C Turner, Maxim Bazhenov and Gilles Laurent. *Olfactory representations by Drosophila mushroom body neurons.* J Neurophysiol, vol. 99, no. 2, pages 734–46, February 2008. 4

[Tzingounis 2007] A. Tzingounis, M. Kobayashi, K. Takamatsu and R. Nicoll. *Hippocalcin Gates the Calcium Activationof the Slow Afterhyperpolarization inHippocampal Pyramidal Cells.* Neuron, vol. 53, pages 487–493, 2007. 16

[van Vreeswijk 1994] Carl van Vreeswijk, L. F. Abbott and G. Bard Ermentrout. *When inhibition not excitation synchronizes neural firing.* Journal of Computational Neuroscience, vol. 1, no. 4, pages 313–321, 1994. 42

[van Vreeswijk 2000] C. van Vreeswijk. *Analysis of the asynchronous state in networks of strongly coupled oscillators.* Phys Rev Lett, vol. 84, no. 22, pages 5110–5113, May 2000. 42, 47 [van Vreeswijk 2010] Carl van Vreeswijk. *Stochastic Models of Spike Trains.* In Analysis of Parallel Spike Trains, Springer Series in Computational Neuroscience. Springer, 2010. 26

[Vere-Jones 2005] D. Vere-Jones and D. J. Daley. An introduction to the theory of point processes: Volume i: Elementary theory and methods: 1. Springer, Berlin, 2. auflage. édition, June 2005. 18

[Vinje 2000] William E. Vinje and Jack L. Gallant. *Sparse Coding and Decorrelation in Primary Visual Cortex During Natural Vision.* Science, vol. 287, no. 5456, page 1273, February 2000. 32

[Vinje 2002] William E. Vinje and Jack L. Gallant. *Natural Stimulation of the Non-classical Receptive Field Increases Information Transmission Efficiency in V1.* The Journal of Neuroscience, vol. 22, no. 7, pages 2904 –2915, April 2002. 46

[Wang 1998] Xiao-Jing Wang. *Calcium coding and adaptive temporal computation in cortical pyramidal neurons.* J Neurophysiol, vol. 79, pages 1549–1566, 1998. 1, 16

[Wehr 1996] Michael Wehr and Gilles Laurent. *Odour encoding by temporal sequences of firing in oscillating neural assemblies.* Nature, vol. 384, no. 6605, pages 162–166, November 1996. 35, 42

[Williams 1997] Sylvain Williams, Mauro Serafin, Michel Mühlethaler and Laurent Bernheim. *Distinct Contributions of High- and Low-Voltage-Activated Calcium Currents to Afterhyperpolarizations in Cholinergic Nucleus Basalis Neurons of the Guinea Pig.* The Journal of Neuroscience, vol. 17, no. 19, pages 7307 –7315, October 1997. 1

[Willmore 2001] B. Willmore and D. J. Tolhurst. *Characterizing the sparseness of neural codes.* Network: Computation in Neural Systems, vol. 12, no. 3, pages 255–270, 2001. 38, 41

[Wold 1954] H. Wold. A study in analysis of stationary time series. Almquist and Wiksell, Stockholm, 1954. 17

[Wüstenberg 2004] Daniel G. Wüstenberg, Milena Boytcheva, Bernd Grünewald, John H. Byrne, Randolf Menzel and Douglas A. Baxter. *Current- and Voltage-Clamp Recordings and Computer Simulations of Kenyon Cells in the Honeybee.* Journal of Neurophysiology, vol. 92, no. 4, pages 2589 –2603, October 2004. 33, 47

[Yamada 2004] Shin-Ichiro Yamada, Hajime Takechi, Izumi Kanchiku, Toru Kita and Nobuo Kato. *Small-Conductance Ca2+-Dependent K+ Channels Are the Target of Spike-Induced Ca2+ Release in a Feedback Regulation of Pyramidal Cell Excitability.* Journal of Neurophysiology, vol. 91, no. 5, pages 2322 –2329, May 2004. 1

[Zacksenhouse 1998] M. Zacksenhouse, D.H. Johnson, J. Williams and C. Tsuchitani. *Single-neuron modeling of LSO unit responses.* J. Neurophysiol., vol. 79, pages 3098–3110, 1998. 16

[Zetzsche 1990] C. Zetzsche. *Sparse coding: the link between low level vision and associative memory.* Parallel processing in neural systems and computers, pages 273–276, 1990. 32